

# The Lorentz gas: A paradigm for nonequilibrium stationary states

C. P. Dettmann  
Rockefeller University, 1230 York Ave, New York NY 10021, USA

July 15, 1999

## Abstract

Nonequilibrium stationary states form the building blocks of more complicated nonequilibrium systems as they define the transport coefficients appearing in the hydrodynamic equations. Recently, many connections have been made between the microscopic dynamical properties of such systems and the macroscopic transport. Although it is often difficult to visualise or understand the dynamics of systems with many particles, it turns out that the Lorentz gas, a system containing only one moving particle, provides a paradigm with which many of these connections can be exhibited and studied. This article surveys the properties of nonequilibrium stationary states, from thermodynamics to the computation of transport coefficients, demonstrating how the Lorentz gas appears as one of the simplest models. A number of current approaches are considered, including linear response formulae applied to equilibrium systems, thermostatted systems and boundary driven systems. All of these and the connections between them can be understood in some detail using the Lorentz gas.

## Contents

<b>1</b>	<b>Why a paradigm?</b>	<b>2</b>
<b>2</b>	<b>Thermodynamics</b>	<b>3</b>
2.1	The second law and nonequilibrium stationary states . . . . .	3
2.2	The Clausius entropy . . . . .	5
2.3	Entropy production . . . . .	6
<b>3</b>	<b>Statistical mechanics</b>	<b>7</b>
3.1	The Boltzmann entropy . . . . .	7
3.2	The Boltzmann transport equation . . . . .	9
3.3	The random Lorentz gas . . . . .	9
3.4	The Gibbs entropy . . . . .	13

<b>4</b>	<b>Equilibrium molecular dynamics</b>	<b>15</b>
4.1	Numerical methods . . . . .	15
4.2	The periodic Lorentz gas . . . . .	19
4.3	Green-Kubo relations . . . . .	20
<b>5</b>	<b>Nonequilibrium molecular dynamics</b>	<b>23</b>
5.1	Introduction to thermostats . . . . .	23
5.2	Gaussian and Nosé-Hoover thermostats . . . . .	24
5.3	The nonequilibrium Lorentz gas . . . . .	26
5.4	Symplectic properties . . . . .	30
5.5	Periodic orbit approaches . . . . .	34
5.6	Nonlinear response . . . . .	37
<b>6</b>	<b>Boundary driven systems</b>	<b>40</b>
6.1	Open boundaries: The escape rate formalism . . . . .	40
6.2	Flux boundaries . . . . .	42
6.3	Boundaries with thermostats . . . . .	43
<b>7</b>	<b>Outlook</b>	<b>44</b>

## 1 Why a paradigm?

Equilibrium statistical mechanics has always been associated with dynamical properties such as ergodicity and mixing [1], although proofs of such properties have been made only recently, and are mostly restricted to billiard and hard ball systems [2]. The advent of the computer has made visualisation and simulation of many kinds of systems possible, inspiring theoretical advances in nonlinear dynamical systems, statistical mechanics, and the relationship between them (and maybe also detrimental effects, Sec. 1.1 of [3]). Dynamical systems theory has benefited from Ruelle’s thermodynamic formalism [4] and Feigenbaum’s renormalisation approach to the bifurcation cascade [5], while dynamics in its turn elucidates the foundations of statistical mechanics [6, 7].

At the heart of the connection between dynamical systems and statistical mechanics lies a paradox. Statistical mechanics is a theory of large systems, valid in the limit as the number of particles (or spins, etc) approaches infinity. Statistical treatments of small systems lack the ensemble equivalence and automatic averaging characteristic of large systems. On the other hand, dynamical systems are most understood in up to three phase space dimensions, due to easier visualisation and topological properties. Systems of infinite extent and number of particles are excluded from the usual definition of a dynamical system, and in any case are difficult to visualise and simulate.

The paradox can be resolved, at least partly, in a number of ways: Real macroscopic systems have a finite number of degrees of freedom, even if that number is large; many of the results connecting dynamic and thermodynamic properties (see below) apply to large as well as small systems; Gallavotti and

Cohen [8, 9] conjecture that the physically relevant properties of systems with many degrees of freedom are those of strongly chaotic dynamics in the sense of Anosov; a turbulent fluid at the onset of chaos has effectively only a few degrees of freedom; numerical methods use a finite number of particles with periodic boundary conditions to simulate an infinite homogeneous system.

Most macroscopic systems, however, have many effective degrees of freedom. The chaotic properties of such systems can be difficult to visualise, and the building blocks of a dynamical description such as Markov partitions and periodic orbits are all but impossible to construct. It is thus difficult to develop a useful intuition and make predictions without some intermediate example, sharing both the properties of chaotic dynamics and of the large systems of interest, without the complexity of many degrees of freedom. Another advantage of such an illustration is that it is possible to investigate the distinction between macroscopic properties that are related to chaotic dynamics, and those that are due to many degrees of freedom.

The discussion thus far has included both equilibrium and nonequilibrium systems. This article focuses on nonequilibrium stationary states for which a natural paradigm is the Lorentz gas. The Lorentz gas can be represented as a two dimensional chaotic map and also exhibits transport in the form of diffusion. The main alternative, discussed in [10], is a class of models based on Baker maps which are exactly solvable, but have less relation to the physical processes they are designed to mimic.

Section 2 outlines the physics of nonequilibrium steady states, introducing the central concepts of entropy production and irreversibility. Section 3 gives statistical definitions of entropy, and how the random Lorentz gas appears naturally as a model of dilute fluids. Section 4 explores computational techniques for systems of many particles, from which the periodic Lorentz gas appears as the simplest example. Section 5 discusses thermostatted models of nonequilibrium stationary states and how results for the Lorentz gas can be applied to such models and hence to systems with many degrees of freedom. Section 6 discusses open models of nonequilibrium stationary states, and their connection to thermostatted models. Finally, section 7 covers the limitations of the Lorentz gas paradigm and outlook for the future.

## 2 Thermodynamics

### 2.1 The second law and nonequilibrium stationary states

An empirical observation is that it is impossible to convert thermal energy of a system into work without affecting the environment, the second law of thermodynamics. Conversely, there are many processes that convert work into thermal energy without affecting the environment, so these are irreversible. It is possible to extract work from a warmer and a cooler subsystem (this is frequently achieved in electricity generation). Thus it is not possible to separate a uniform system into warmer and cooler parts without the addition of work, as this would

permit the extraction of work from the thermal energy of the original system. Conversely, the spontaneous flow of thermal energy from a warmer to a cooler subsystem without the extraction of work is also an irreversible process.

Many irreversible processes, including mutual diffusion of different particle species, electric current flowing through a resistor, shear flow of a viscous fluid and heat conduction can occur in such a way that macroscopic variables including the various forces and fluxes are independent of time in a region of interest. Such a system is said to be in a nonequilibrium stationary state. Two properties should be noted immediately:

1. Due to the irreversible processes, the region is necessarily in contact with an environment which is not truly stationary. For example, a resistor continually depletes its voltage source as well as heating its environment. Conceptual difficulties can arise when the environment is either ignored or assumed to be infinite and hence unaffected by contact with the region of interest.
2. The stationarity is of a statistical kind, as is usual when dealing with systems with many degrees of freedom. The individual particles are not stationary, leading to statistical fluctuations in macroscopic quantities, although these are often small when very many particles are involved. Statistical stationarity is quantified in terms of ensembles, or probability distributions on phase space, that may be stationary as determined by the dynamics and boundary conditions. This distinction between the properties of individual realisations and ensembles is particularly striking in systems with few degrees of freedom, such as the Lorentz gas, where the fluctuations are very large.

When the driving forces (concentration gradient, electric field, shear stress or temperature gradient) in the above examples are set to zero, there are no longer any irreversible processes, and the steady state of the system is an equilibrium state similar to that of an isolated system. The only difference would be due to the interaction with the environment, which appears in the ensembles of equilibrium statistical mechanics. The microcanonical ensemble of an isolated system is equivalent (in the limit of many particles) to the canonical ensemble of a system in thermal contact with its environment. An equilibrium state may not be unique, for example a substance that is a crystalline solid at a certain temperature may have its axes in many possible orientations.

When the driving forces are very small compared to relevant physical scales so that, for example, the relative variation of all quantities is much less than unity over a distance equal to the mean free path, the steady state is said to be close to equilibrium. Linear response theory may be applied, leading to fluxes (particle current, electric current, strain rate or heat flux) proportional to the forces. The constants of proportionality (diffusion coefficient, electrical conductivity, shear viscosity or thermal conductivity) are known as linear transport coefficients. They appear in macroscopic descriptions such as the Navier-Stokes

equations. Mathematical proofs of their existence have been given for some small systems [11].

A steady state need not be close to equilibrium, and such states show a rich range of phenomena, as we will see in the Lorentz gas. There may be nonlinear relationships between the fluxes and forces, but the concepts themselves change as properties no longer resemble those of an equilibrium system. A viscous system shearing sufficiently so that nonlinear terms become important will also be generating enough heat for thermal conduction effects to contribute. Higher shear rates correspond to an increasing Reynolds number, leading to turbulence. There is in general no guarantee of uniqueness or even existence of a nonequilibrium steady state.

Another problematic aspect of far from equilibrium steady states is the difficulty in defining a thermodynamic limit, where the number of particles, volume, and other extensive variables go to infinity such that their ratios are finite. The presence of strong gradients rapidly causes huge variations in temperature, density, and so on, leading to physically unrealistic scenarios. This difficulty is solved in the linear regime by demanding that the variations in such quantities remain fixed, so that their gradients approach zero in the thermodynamic limit.

There are a number of equivalent statements of the second law, and as many approaches to the related issues of irreversibility and entropy as there are texts on thermodynamics. Some of the more important ideas are sketched below with their relation to the Lorentz gas and nonequilibrium stationary states.

## 2.2 The Clausius entropy

Just as the notion of temperature can be understood in a qualitative manner from the direction of the flow of thermal energy, it is clear that the existence of irreversible processes implies that there is a property of the system, namely the entropy, that remains constant in reversible processes and increases in irreversible processes. A unique state of maximum entropy then corresponds to equilibrium, because there are no more states to which the system can go. We will usually assume (quite reasonably for fluids, at least) that there is only one equilibrium state for given constants of the motion (energy, number of particles, volume) corresponding to maximal entropy.

Historically the first quantitative statement in this direction, due to Clausius, defines the change in entropy as a system moves quasistatically from one equilibrium state to another. Specifically,

$$\Delta S_C = \int \frac{dq}{T} \tag{1}$$

where  $S_C$  is the entropy (defined up to an additive constant),  $T$  is the temperature, and  $q$  is the thermal energy injected into the system from a thermal reservoir at the same temperature as the system. “Quasistatically” means a limit in which all time derivatives approach zero. It disallows processes such as the free expansion of a gas when a partition is removed; such processes are inherently irreversible. The temperature can be defined from the equation of

state of an ideal (in practice, dilute) gas, that is, proportional to the pressure times the volume. Alternatively, if we equate  $S_C$  with one of the statistical mechanical entropies discussed below, the temperature is then defined from Eq. (1) or its equivalent.

Note that the thermodynamic definition of entropy only makes sense for a system at or very close to equilibrium. Once we know the entropy of a particular substance as a function of temperature (or energy density) and pressure (or mass density) at equilibrium, the definition can be extended to systems in “local equilibrium”, including stationary states close to equilibrium, by assuming the extensive property, that is, the total entropy of a system is equal to the sum of the entropies of its subsystems, and that the subsystems can be considered close to an equilibrium state.

Extensivity is expected classically when interactions between the particles are short ranged, which is usually the case. In the large system limit, the interactions reduce to boundary terms which are much smaller than the bulk effects. Notable exceptions to extensivity include some quantum systems (for example Bose-Einstein condensation) and gravitational systems (for example black holes). When there are strong interactions between subsystems it does not make sense to consider the Clausius entropy of the subsystems.

### 2.3 Entropy production

It is possible to apply the above prescription to nonequilibrium stationary states that are close to equilibrium. The entropy of the region under consideration does not vary with time, due to stationarity. However, the irreversible processes cause an overall increase, or production of entropy, so that thermal energy released into the environment increases its total entropy. Thus we have

$$0 = \dot{S}_{\text{ness}} = \dot{S}_{\text{irr}} + \dot{S}_{\text{in}} \quad (2)$$

where  $\dot{S}_{\text{ness}}$  corresponds to the nonequilibrium steady state,  $\dot{S}_{\text{irr}}$  is the irreversible entropy production, and  $\dot{S}_{\text{in}}$  is the (negative) flow of entropy in from the environment. Such entropy balance equations figure prominently in the Baker map approaches [10] in various notations. The irreversible entropy production and entropy flux are also independent of time from stationarity,

$$\ddot{S}_{\text{irr}} = 0 = \ddot{S}_{\text{in}} \quad (3)$$

The origins of the entropy flux  $\dot{S}_{\text{in}}$  depends on the nature of the system. An electric current density  $\mathbf{J}$  is driven by an electric field  $\mathbf{E}$  that does work but does not affect the entropy. This work is converted into an equivalent amount of thermal energy that then leaves the system, taking with it an entropy flux given by (1). Thus we have

$$\dot{S}_{\text{irr}} = -\dot{S}_{\text{in}} = \frac{\mathbf{J} \cdot \mathbf{E}V}{T} \quad (4)$$

where  $V$  is the volume. Similar considerations hold for shear flow. In the case of heat conduction,  $\dot{S}_{\text{in}}$  contains contributions from heat (and hence entropy) flow

in from a higher temperature and out to a lower temperature. The amounts of heat are equal since energy is balanced, but more entropy flows out owing to the different temperatures in the denominator. Entropy is also produced when two substances mutually diffuse; see the discussion on the Gibbs mixing paradox in Sec. 3.4 below. The connection between mutual diffusion and heat flow is more difficult to understand, but it is clear that work or a temperature differential is required to separate a mixture. Whatever the situation, the entropy production is always the product of a force and a flux. The second law, which requires positive entropy production, thus determines that transport coefficients (the quotient of a flux and force) are positive.

For steady states far from equilibrium, it is not clear how to calculate the entropy from (1) since there is no equilibrium state with which to compare the system. However, if it is possible to couple the system reversibly to a thermal reservoir close to equilibrium, all of the above arguments remain valid so the entropy production can be calculated from the forces and fluxes as above. There are some possible pitfalls to this approach, for example some steady states far from equilibrium have different effective temperatures for particles moving in different directions. This makes it difficult to imagine how to construct the required thermal reservoir in principle, let alone in practice. Typically such details are ignored, the above equations are applied, and an additional postulate is added to the theory.

## 3 Statistical mechanics

### 3.1 The Boltzmann entropy

Now we turn to the statistical viewpoints of Boltzmann and Gibbs. The macroscopic thermodynamic variables fluctuate due to microscopic movement of the molecules, with the exception of exactly conserved quantities such as the energy of an isolated system. This means that, for example, the second law of thermodynamics is not always valid. The local temperature (as measured by the average kinetic energy over a small region) of an equilibrium system fluctuates, leading to a transition from a state with uniform temperature to a state with slight variations in temperature. However, large fluctuations as measured by a large decrease in entropy are very rarely observed.

In order to quantify the frequency of certain fluctuations, and because we do not have precise information about the positions and momenta of macroscopic numbers of particles (and also for reasons related to quantum mechanics, which we shall ignore here), it makes sense to describe a system in terms of probabilities. Probabilistic assumptions about the initial conditions of the microscopic particles can also explain the paradox of irreversibility, how the second law of thermodynamics is compatible with perfectly reversible Newtonian microscopic equations of motion. The time reverse of a dissipative process shows large violations of the second law, but is not observed because the initial conditions are not very probable for some reason, depending on the physical or philosophical

justification of the probabilistic assumptions of the theory.

For Hamiltonian systems with, say,  $N$  particles moving in  $d$  dimensions, the most natural probability measure on the  $2Nd-1$  dimensional surface of constant energy  $\Gamma$  is the (restricted) Lebesgue measure  $d\Gamma = \delta(H - E)dx^{Nd}dp^{Nd}/h^{Nd}$ , the postulate of equal a priori probability. In the nineteenth century the only real justification for this was the theorem of Liouville that this measure is preserved by Hamiltonian dynamics (see Sec. 3.4). Ergodicity implies that this measure does indeed give the correct time averages, but the time required for a system to closely approach all points in the phase space with even very coarse precision is astronomical for systems with many degrees of freedom. See [1] for a more detailed discussion of ergodicity. Many of the current models of nonequilibrium stationary states do not preserve Lebesgue measure, so other invariant measures are more appropriate, and will be discussed later. The above measure is normalised by powers of Planck's constant  $h$  for dimensional reasons. This particular normalisation can be justified in quantum mechanics, but here we note that it sets the (classically) arbitrary additive constant associated with the entropy.

The Boltzmann definition of entropy considers that for each configuration of macroscopic system variables  $X$ , there is a region in microscopic phase space of volume  $\int_X d\Gamma$ . Then the entropy corresponding to the configuration is

$$S_B(X) = k_B \ln \int_X d\Gamma \quad (5)$$

where  $k_B$  is Boltzmann's constant and has dimensions of an energy divided by a temperature, see (1). The idea is that a system will be most likely to move to one of the very large regions of phase space corresponding to greater entropy. The probability of finding the system in a given state is thus proportional to  $\exp[-(S_0 - S_B)/k_B]$  which is virtually zero for a large system not in its maximum entropy state  $S_0$  since the entropy is proportional to the number of particles. The Boltzmann entropy of a unique equilibrium state is thus the logarithm of the volume of the whole surface of constant energy, and agrees with the Clausius definition in the cases where they can be compared, that is, equilibrium systems with many particles. Boltzmann's entropy and its relation to irreversible processes is discussed in Ref. [12].

In order to apply this to nonequilibrium steady states, decisions must be made about the most natural phase space for a system in contact with its environment (discussed extensively below) as well as the correct measure to use. In this context it should be noted that recent papers of Rugh using the Boltzmann entropy to define a dynamical temperature for Hamiltonian systems [13, 14] have been applied to nonequilibrium systems [15] by means of the Hamiltonian formulation of the isokinetic thermostat (Ref. [16], see Sec. 5.4 below), and also to identify the heat flow in systems with inhomogeneous shear [17]. Apart from this, most application of entropy to nonequilibrium steady states seems to be closer in spirit to the Gibbs approach, Sec. 3.4.

### 3.2 The Boltzmann transport equation

Another type of statistical assumption appears in the Boltzmann equation which describes dilute gases at or away from equilibrium. The quantity of interest is the single particle distribution function  $f(\mathbf{x}, \mathbf{v}, t)$  which gives the probability density of finding a particle with the given position and velocity at a certain time. A straightforward derivation based on the equations of motion gives

$$\frac{\partial f}{\partial t} + \mathbf{v} \cdot \nabla_{\mathbf{x}} f + \frac{1}{m} \mathbf{F}_e \cdot \nabla_{\mathbf{v}} f = \Gamma_{coll} \quad (6)$$

where  $m$  is the mass,  $\mathbf{F}_e$  is the external force on each particle, and the term on the right hand side denotes the effect of the collisions between particles.

For a dilute gas without long range interactions between the particles, only two-body collisions contribute, however an exact treatment requires the two-particle distribution function  $f_2(\mathbf{x}_1, \mathbf{x}_2, \mathbf{v}_1, \mathbf{v}_2, t)$  which gives the joint probability of two particles entering a collision. The assumption made by Boltzmann, called the stosszahlansatz, consists of replacing the two-particle distribution by the product of two one-particle distribution functions, thus assuming that the particles entering the collision are uncorrelated.

Boltzmann showed in his celebrated H-theorem that a certain quantity,

$$H(t) = \int dx dv f(\mathbf{x}, \mathbf{v}, t) \ln f(\mathbf{x}, \mathbf{v}, t) \quad (7)$$

never increases as  $f$  evolves under (6) with the stosszahlansatz. In fact,  $-k_B H$  can be identified with the entropy (up to an additive constant), and Boltzmann argued that this was a derivation of the second law.

The Boltzmann equation describes a dilute gas approaching equilibrium well, but the addition of this statistical assumption has the effect of ignoring the fluctuations that are known to occur. The solution of the Boltzmann equation can never return to a state of smaller entropy, despite the fact that this is known to happen occasionally. For this reason, the statistical assumptions going into the Boltzmann equation, although useful for calculating the properties of nonequilibrium gases, are not viewed as a fundamental explanation of the second law. See Ref. [18] for further discussion.

### 3.3 The random Lorentz gas

The Boltzmann equation is a nonlinear integro-differential equation, and as such it cannot be solved in most cases without making restrictive and sometimes physically obscure approximations. One case that illustrates the properties of the Boltzmann equation well, while remaining simple enough to solve is the random Lorentz gas [19, 20].

The random Lorentz gas can be motivated on physical grounds as follows: Suppose we have a dilute gas in equilibrium, consisting of a mixture of two species. Both are spheres (or in two dimensions, disks) that are rigid (so any internal degrees of freedom are ignored), and hard (so the range of interaction is

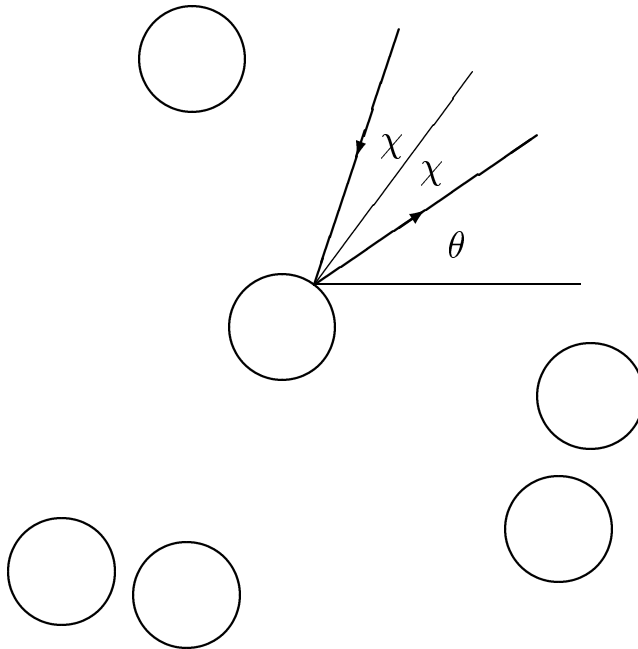


Figure 1: The random Lorentz gas. In the Lorentz Boltzmann equation (10) below, the particle arrives in direction  $\theta$  from direction  $\pi + \theta + 2\chi$ .

much smaller than other length scales) with one much larger and heavier than the other, and with number densities (number per unit volume) such that there are many more smaller particles, but almost all collisions are between smaller and larger particles, rather than among the smaller particles. Thus for masses  $m_S$  and  $m_L$ , radii  $r_S$  and  $r_L$ , number densities  $n_S$  and  $n_L$  and dimension  $d$  we require  $m_S \ll m_L$ ,  $r_S \ll r_L$ ,  $n_S \gg n_L$  and  $n_S r_S^{d-1} \ll n_L r_L^{d-1}$ . The equipartition of energy implies that at equilibrium, the average kinetic energy of each particle is equal, hence the larger particles have much smaller velocities. In this limit we have a large number of noninteracting pointlike particles colliding with fixed, randomly placed spherical (or circular) obstacles. The magnitude of the velocity is a constant of the motion, and changing the velocity is equivalent to scaling the time, so we can restrict ourselves to the case of unit velocity, averaging over the velocity distribution later if necessary. Similarly, scaling the distance permits us to set the radius of the scatterer equal to unity (there are other conventions possible, such as setting the mean free path to unity). We thus have a model with one free parameter, the number density of scatterers  $n$ , called the random Lorentz gas. See Fig. 1.

The designation “random” comes from the placement of the scatterers; a periodic placement appears naturally from the methods of molecular dynamics, and is discussed in Sec. 4.2. From a mathematical point of view, it can be assumed that a random placement ensures that there is no exact relation between the positions of the scatterers. It is possible to consider an average over

all such random configurations, however this is generally unnecessary since any given finite arrangement of scatterers appears to arbitrary precision somewhere in an infinite arrangement. A random configuration drawn from the correct distribution can be obtained on a computer by a variant of the Metropolis algorithm [21], in which any initial arrangement (perhaps periodic) is modified by a large fixed number of attempted random shifts of randomly chosen scatterers; any illegal shift resulting in overlapping scatterers is rejected, and the configuration is unchanged. Note that the number of attempted random shifts is fixed, not the number of successful shifts. As a model in its own right (but not for Boltzmann equation approaches), the dilute condition (not included above,  $n_L r_L^d \ll 1$ ) may be relaxed. It is also possible to consider a model where the scatterers are permitted to overlap.

Before returning to the Boltzmann equation, and hence the low density limit, we note an exact result that holds for all densities, that is, the mean free time between collisions (or distance, since the velocity is one). The mean free time can be computed exactly for all billiard systems [22], and this calculation can be applied to the (infinite) Lorentz gas by carefully taking a large system limit. Briefly, the argument is that the total volume of phase space can be computed in two ways, one by subtracting the volume of the scatterers from the total volume, and the other by considering the mean path length over each point on the boundary. The result in two dimensions is

$$\bar{\tau} = \frac{\pi|Q|}{|\partial Q|} = \frac{1}{2n} - \frac{\pi}{2} \quad (8)$$

and in three dimensions is

$$\bar{\tau} = \frac{4|Q|}{|\partial Q|} = \frac{1}{\pi n} - \frac{4}{3} \quad (9)$$

where  $|Q|$  is the volume of the billiard and  $|\partial Q|$  its boundary. The last equality in each case corresponds to the non-overlapping Lorentz gas with  $n$  scatterers per unit volume. It is always positive;  $n$  can never be larger than the close-packed values. These formulas are valid regardless of the locations of the scatterers, so they apply to both the random and the periodic Lorentz gas as long as the scatterers do not overlap.

The Boltzmann equation for the Lorentz gas in the low density limit is linear, because the probability distribution of one of the objects involved in a collision (the fixed scatterer) is constant. For example, in two dimensions we have for the single particle distribution function  $f(x, y, \theta, t)$  where  $\theta \in \mathbf{R}/2\pi\mathbf{Z}$  is the direction of the velocity:

$$\begin{aligned} & \left( \frac{\partial}{\partial t} + \cos \theta \frac{\partial}{\partial x} + \sin \theta \frac{\partial}{\partial y} \right) f(x, y, \theta, t) \\ &= \int_{-\pi/2}^{\pi/2} f(x, y, \pi + \theta + 2\chi) n \cos \chi \, d\chi - 2nf(x, y, \theta, t) \end{aligned} \quad (10)$$

Here, the external force in (6) is zero, and the right hand side contains two terms giving the rate of particles entering and leaving a given velocity direction, see Fig. 1. Without explicitly solving the equation, it can be seen that the effect of the collision operator is to redistribute the  $2nf$  to the other velocity directions, making the distribution flatter and smoother. We can immediately write down a solution in the form

$$f(x, y, \theta, t) = \sum_{m=-\infty}^{\infty} f_m \exp(ik_x x + ik_y y + im\theta - \gamma t) \quad (11)$$

which is substituted to obtain

$$(\gamma_m - \gamma)f_m + \frac{ik_x + k_y}{2}f_{m-1} + \frac{ik_x - k_y}{2}f_{m+1} = 0 \quad (12)$$

with

$$\gamma_m = \frac{8nm^2}{4m^2 - 1} \quad (13)$$

the decay rates of the modes in the homogeneous case ( $k_x = k_y = 0$ ). Perturbing the homogeneous zero mode with small  $k_x$  and  $k_y$  we obtain a “dispersion” relation

$$\gamma_0(k) = D_2 k^2 + O(k^4) \quad (14)$$

with the diffusion coefficient in two dimensions given by

$$D_2 = \frac{3}{16n} . \quad (15)$$

In three dimensions the diffusion coefficient is

$$D_3 = \frac{1}{3\pi n} . \quad (16)$$

For general dilute gases, in which the Boltzmann equation cannot be solved exactly, the diffusion coefficient is obtained by the Chapman-Enskog methods of standard kinetic theory [23], for which the random Lorentz gas provides a useful pedagogical example. More calculations and relations involving the diffusion coefficient of the Lorentz gas are given in later sections. A Boltzmann-like equation for the Lorentz gas has also been applied to a dynamical problem, that of computing the Lyapunov exponents and the Kolmogorov-Sinai entropy, see [24] for a detailed discussion.

At higher densities the Boltzmann equation is no longer a good approximation, and the physics changes due to the appearance of power law decay in the correlation functions, the “long time tails”, both for the random Lorentz gas and more general gases [20, 25]. The Lorentz gas has a velocity autocorrelation function decaying as  $t^{-d/2+1}$ , sufficient to lead to nonanalytic higher terms in Eq. (14), see Secs. 4.3, 5.6 and Refs. [20, 26].

We leave the random Lorentz gas at this point to continue our discussions of entropy in nonequilibrium stationary states, but it is worth noting that many of the results obtained in connection with molecular dynamics and the periodic Lorentz gas in later sections also apply to the random case.

### 3.4 The Gibbs entropy

The other statistical formulation of the entropy we will consider is due to Gibbs. Given an arbitrary smooth probability density  $\rho(\Gamma)$  on phase space the Gibbs entropy is defined as

$$S_G = -k_B \int \rho(\Gamma) \ln \rho(\Gamma) d\Gamma . \quad (17)$$

This is similar to the Boltzmann H function of Eq. (7) except that  $\rho$  is defined on the whole of accessible phase space compared with the single particle distribution function  $f$ . The accessible phase space  $\Gamma$  could be the constant energy surface of an isolated system, but will be generalised below when other ensembles are discussed.

The Gibbs entropy is also extensive (Sec. 2.2) if it is noted that when there are  $N$  identical particles, the phase space is a subset of  $\mathbf{R}^{2Nd}/\mathbf{S}_N$  where  $\mathbf{S}_N$  is the permutation group of order  $N$ . In terms of the standard “unreduced” phase space (which is easier to compute with) this means multiplying  $\rho$  by a factor  $N!$  when the particles are indistinguishable. The difference between the entropy of identical and distinguishable particles is called the entropy of mixing. It solves the Gibbs paradox which notes that mixing of identical substances has no effect, while mixing of different substances (without extraction of work) is an irreversible process. In other words, self diffusion is not associated with an increase in entropy, and is not observable without artificial means such as a “tagged particle”, whereas mutual diffusion is a true irreversible process, associated with an increase in entropy and directly observable.

This is relevant to the Lorentz gas in that when the Lorentz gas is considered to be a mixture of two different species (as in Sec. 3.3) there is an entropy production associated with the diffusion coefficient, and when it is considered to be a model of one species (as in Sec. 4.2) there is no entropy production involved. The physics of entropy production is thus connected to the interpretation of the model rather than anything in the model itself, such as the equations of motion. This illustrates the need for caution whenever establishing an equivalence between features of the model and physical reality.

The Gibbs entropy can be used to derive the ensembles of equilibrium statistical mechanics as follows: The maximum entropy (subject to normalisation of the probability) corresponding to the equilibrium state of an isolated system is attained when  $\rho$  is a constant, consistent with the postulate of equal a priori probability, Sec. 3.1. If the system can exchange energy with the environment, the constant energy constraint on phase space is replaced by an average energy constraint on  $\rho$ ,

$$\langle E \rangle = \int E(\Gamma) \rho(\Gamma) d\Gamma \quad (18)$$

in addition to conservation of probability. The extra constraint when maximising the Gibbs entropy gives a Lagrange multiplier which turns out to be related

to the temperature. In this manner the canonical ensemble

$$\rho(\Gamma) = \exp\left(\frac{-E}{k_B T}\right) \quad (19)$$

is derived. Similarly, when the system can exchange particles with the environment, the constraint of fixed  $N$  is replaced by a Lagrange multiplier which is related to the chemical potential  $\mu$ , and the phase space is expanded to include all numbers of particles. For more details see for example Ref. [27]. In general, for each constant of the motion (in a general sense)  $E$ ,  $N$  and volume  $V$  there is a thermodynamic conjugate variable  $T$ ,  $\mu$  and the pressure  $p$  respectively.

Given its success in equilibrium statistical mechanics, the possibility of extending the phase space to allow for interactions with the environment, and the appearance of conjugate variables analogous to the conjugate forces and fluxes of irreversible thermodynamics (Sec. 2.3), it would seem that the Gibbs entropy is the natural candidate for extension to nonequilibrium systems. Unfortunately there is one major obstacle, which we now discuss.

Suppose an isolated system with phase point  $\Gamma$  has equations of motion

$$\frac{d\Gamma}{dt} = F(\Gamma) \quad (20)$$

then the Liouville equation for a probability density  $\rho(\Gamma)$  is

$$\frac{\partial \rho}{\partial t} + \nabla \cdot (F\rho) = 0 \quad (21)$$

and hence (after two partial integrations)

$$\frac{dS_G}{dt} = k_B \int (\nabla \cdot F)\rho d\Gamma \ . \quad (22)$$

For a Hamiltonian system

$$\nabla \cdot F = \nabla_q \cdot \dot{q} + \nabla_p \cdot \dot{p} = \nabla_q \cdot \nabla_p H - \nabla_p \cdot \nabla_q H = 0 \quad (23)$$

so both the phase space volume and the Gibbs entropy are constants of the motion:

$$\frac{d\rho}{dt} = \frac{\partial \rho}{\partial t} + F \cdot \nabla \rho = 0 \quad (24)$$

$$\frac{dS_G}{dt} = 0 \quad (25)$$

The Gibbs entropy as it stands cannot explain the second law of thermodynamics.

The reason behind this becomes clear as we realise that a Hamiltonian system (or any system with phase space volume conservation) moves probability density around, but does not alter its initial values. If the system has chaotic dynamics (say, mixing), an initially smooth distribution will be stretched and folded to

become rapidly varying in the stable directions, but remains continuous for all times. The Gibbs entropy gives minus the amount of information (in the sense of information theory) we have about the state of the system, and this information does not change under incompressible time reversible deterministic dynamics.

It is clear that any observation of a real system is uncertain to some degree, so that from the point of view of measuring the system, a rapidly varying probability distribution may be replaced by its average over the scale of resolution. This procedure is called coarse graining, and the smoother distributions generated by such a procedure have a higher entropy than the initial distributions. Like the Boltzmann entropy, for which the definition of the state  $X$  is somewhat arbitrary, the coarse grained Gibbs entropy depends on the observer. The paradox is that the second law of thermodynamics is valid however (and indeed whether) the system is being observed. Quantum mechanics is not obviously helpful in explaining this dilemma, since the second law is observed in classical computer simulations. A critical review of this issue as applied to recent work along the lines of the thermostatted and open models discussed below (see also Sec. 5.3) concludes:

*The above discussion on the coarse grained approach to a complete dynamical theory of irreversible thermodynamics pointed out difficulties which we found in the current formulations. Therefore it seems that a coarse grained entropy approach based on  $S_G$  does not provide a satisfactory connection with irreversible thermodynamics, ... further study of the connection of the dynamics of particle systems in nonequilibrium states and irreversible thermodynamics is still required. [28]*

## 4 Equilibrium molecular dynamics

### 4.1 Numerical methods

At this point we move from statistical to dynamical descriptions of many particle systems, in particular nonequilibrium stationary states. To construct mathematical models it is helpful to take inspiration from computer algorithms used to study such systems. Aggregates of millions of particles can now be simulated on a computer. In this way, equilibrium and nonequilibrium properties of materials may be computed using any desired intermolecular forces and initial conditions [29, 30, 31]. Compared to analytic calculations, many restrictions such as simplicity of the forces, approximations and assumptions can be eliminated. Compared to experiments, the results are only as good as the model, but it is possible to simulate experimentally inaccessible regimes. Compared to mathematical proofs, the results are usually not rigorous, however while a system may not be proved ergodic (for example), empirical limits may be placed on non-ergodic behaviour, sufficient to determine whether any such non-ergodic behaviour is physically relevant.

It is difficult to put rigorous bounds on the accuracy of numerical simulation results, particularly when the dynamics is exponentially unstable. Often there is a shadowing theorem stating that the numerical trajectory is close to some exact trajectory of the dynamics, however this does not guarantee that the exact trajectory is typical with respect to the desired distribution of initial conditions. Sometimes a simulated low dimensional attractor can result in a periodic orbit due to the finite number of states accessible to the dynamics. The averages and other properties of this periodic orbit are quite different to the dynamics as a whole. In this case, the addition of small amounts of noise to the dynamics often leads to more realistic trajectories, and can actually be used as a mathematical definition of an attractor [32]. When the correlation dimension of the attractor is sufficiently large (for example, 2) precision related periodic orbits are rarely observed, and standard tests such as varying the precision of the calculations usually indicate that the results have probably converged.

The results of numerical simulations are as good as the algorithms used. While attaining optimum speed and accuracy is somewhat of an art form, there are a number of general methods and principles. The equations of motion for simulations are Newton's equations of motion, reducing in the simplest case of  $N$  spherical identical particles to

$$\dot{\mathbf{x}}_i = \frac{\mathbf{p}_i}{m} \quad (26)$$

$$\dot{\mathbf{p}}_i = - \sum_{j \neq i} \frac{\partial \phi(r_{ij})}{\partial \mathbf{x}_i} \quad (27)$$

$$r_{ij} = |\mathbf{x}_i - \mathbf{x}_j| \quad (28)$$

interacting via a specified potential  $\phi$ , which can be calculated from pair correlation data obtained in diffraction experiments.

The Lennard-Jones potential,

$$\phi_{LJ}(r) = 4\epsilon \left[ \left( \frac{\sigma}{r} \right)^{12} - \left( \frac{\sigma}{r} \right)^6 \right] \quad (29)$$

is quite realistic for monatomic fluids such as argon. There are of course more elaborate models involving interactions between three or more particles for specific substances, for example carbon [33], and in principle there are also quantum effects. Here  $\sigma$  and  $\epsilon$  are parameters setting the length and energy scales, respectively. In simulations mass, length and time are scaled so that  $m = \sigma = \epsilon = 1$ . When there is more than one type of particle it is possible to scale the positions, momenta and forces by appropriate factors of the squareroot of the mass in order to remove  $m$  and  $\epsilon$  from the problem, however the differing radii remain intrinsic to the dynamics.

It is sometimes advantageous to eliminate the possibility of bound states generated by the negative part of the potential, and also to make it finite range to shorten the computation. For this reason it is common to use a shifted and

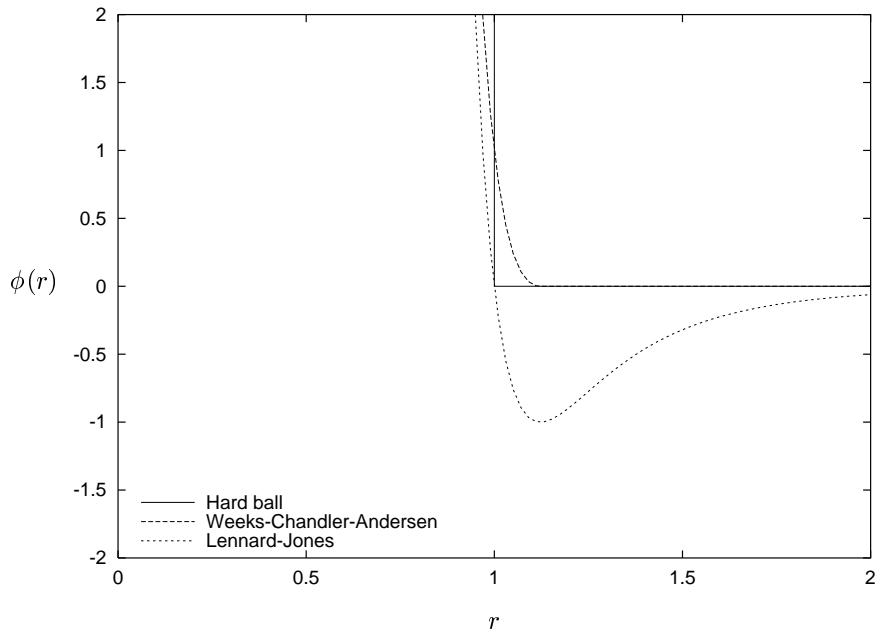


Figure 2: Interparticle potentials, scaled so that  $\sigma = \epsilon = 1$ .

truncated version, called the Weeks-Chandler-Andersen [34] potential,

$$\phi_{WCA}(r) = \begin{cases} \phi_{LJ}(r) + 1 & r < 2^{1/6}\sigma \\ 0 & r > 2^{1/6}\sigma \end{cases} \quad (30)$$

which has a continuous first derivative across the boundary.

Still simpler, and surprisingly realistic at low to moderate densities is the hard ball potential,

$$\phi_{HB}(r) = \begin{cases} \infty & r < \sigma \\ 0 & r > \sigma \end{cases} \quad (31)$$

See Fig. 2. The great advantage of hard potentials for simulations is that the solution of the equations of motion is known, so it is not necessary to use integration routines which are much slower than substitution into an explicit formula and often require relatively small steps for accuracy. The disadvantage from a physical point of view is the absence of a characteristic energy scale, leading to a trivial dependence of thermodynamic quantities on the temperature. Nevertheless, hard ball gases exhibit fairly realistic phase transitions in terms of pressure and density.

The boundary conditions are extremely important for both equilibrium and nonequilibrium simulations. For example, suppose we have  $10^3$  particles in 3 dimensions, so 10 particles in each direction. Suppose also that the boundary conditions are not treated correctly, affecting a boundary layer of one particle.

This is a conservative estimate, since a dilute system would have a longer mean free path and hence a thicker boundary layer. The number of particles not on the boundary is  $8^3 = 512$ . Thus almost half of the particles are affected by a poor choice of boundary conditions in this example.

Often we are interested in the bulk properties of a medium, far from any physical boundary. For these properties the natural boundary conditions are periodic, viewed either as a unit cell infinitely repeated (corresponding to an infinite system with a special symmetry) or as a finite system where particles that exit via one boundary reappear at the opposite boundary. Both viewpoints are useful, depending on what is being discussed. The most common periodic cells for molecular dynamics simulations are either chosen for simplicity (square, cube), or based on a close packed array, particularly for high density (hexagonal, rectangle with side ratio a rational multiple of  $\sqrt{3}$ , similar choices in three dimensions). The hexagonal case is of special interest for the Lorentz gas, as it can lead to a finite horizon, see Sec. 4.2.

It is clear that equilibrium properties can be calculated in this way, but the correct approach to nonequilibrium properties is far from obvious. The many possible schemes of theoretical and/or practical interest may be broadly categorised as follows:

1. Linear response (Green-Kubo) formulae from which linear transport coefficients may be calculated from purely equilibrium simulations.
2. Homogeneous molecular dynamics, where the contact with the environment is simulated by driving forces on each particle, thermostat “frictional” forces, and (for shear flow) “sliding brick” boundary conditions.
3. Inhomogeneous systems driven entirely by boundary effects.
4. Inhomogeneous systems with a combination of boundary effects and bulk effects such as thermostats.

The most efficient methods for calculating the linear transport coefficients are the homogeneous thermostatted approaches, which is what they were designed for. The other approaches nevertheless have a great deal of theoretical interest, including a number of analytic relations between dynamical (microscopic) and thermodynamic (macroscopic) properties.

The calculation of nonequilibrium properties from equilibrium simulations is clearly limited to situations close to equilibrium; beyond linear transport coefficients the response is usually nonanalytic as in Sec. 5.6. For the other approaches, the degree to which far from equilibrium predictions can be made depends on the physics. A system far from equilibrium that remains homogeneous must usually radiate heat (by phonons, photons, neutrinos etc. with long scattering lengths) rather than conduct it. Similarly, boundary driven nonlinear effects are more strongly affected by the choice of boundary conditions than near equilibrium. For reasons such as these, far from equilibrium situations need to be put on a more individual basis, not to say that they don’t share many properties in common.

The remainder of this article discusses a number of these schemes in detail, specifically Green-Kubo formulae and some thermostatted and boundary methods. These are illustrated using the Lorentz gas, from which general properties of nonequilibrium steady states can be understood and discovered, and to which we turn now.

## 4.2 The periodic Lorentz gas

What is the simplest possible molecular dynamics model? If we use periodic boundary conditions, momentum is conserved, so a single particle moves trivially with constant velocity. The simplest interaction potential is the hard ball, Eq. (31). Two identical hard rods in one dimension exchange their velocities on collision, again leading to trivial dynamics. Thus we need two hard disks moving in two dimensions under periodic boundary conditions.

Assuming there is no drift (that is, no centre of mass motion) and moving to relative coordinates, we see that the problem of two hard disks is equivalent to a point particle colliding with a disk with twice the original radius in periodic boundary conditions or (equivalently) on a periodic lattice of such scatterers. This is the periodic Lorentz gas. As a model it differs only from the random Lorentz gas, Sec. 3.3 in the location of the scatterers and possibly whether they overlap, but the interpretation here is quite different.

There are three possible regimes in the periodic Lorentz gas, depending on the shape of the periodic cell and the size of the hard disks, see Fig. 3. Because the reduction to relative coordinates has the effect of doubling the radius, it is possible for the disks in the reduced case to overlap, often leading to a trapped scenario where there is no diffusion. It is possible to define a viscosity however [11]. When the disks do not overlap, it is possible for a hexagonal cell to have an upper bound on the time between collisions, and the Lorentz gas is said to have finite horizon, and there is normal diffusion defined by  $\langle x^2 \rangle \sim t$ , see (35) below and Ref. [35]. This is similar to the random Lorentz gas of Sec. 3.3 which has zero probability of an infinite trajectory, and also normal diffusion. For square, rectangular, and three dimensional cells, non-overlapping disks have an infinite horizon, leading to anomalous diffusion of the form  $\langle x^2 \rangle \sim t \ln t$  (see Refs. [36, 37] for two dimensions).

The periodic cell in two dimensions is usually square, rectangular or hexagonal. In each of these cases, the Lorentz gas is dynamically equivalent to a finite billiard of the same shape and size and with hard wall boundaries. This is because a billiard with reflections at the boundary can be extended by reflecting (rather than translating) the domain across each straight boundary. In addition, the square, rectangle and hexagon are the same whether reflected or translated, so reflecting boundary conditions are equivalent to periodic boundary conditions. Thus the Lorentz gas with a square periodic cell is equivalent to the Sinai billiard, which contains a circular scatterer at the centre of a square billiard.

Common to many models with hard collisions, it is often convenient (also for nonequilibrium extensions discussed below) to consider the natural Poincaré

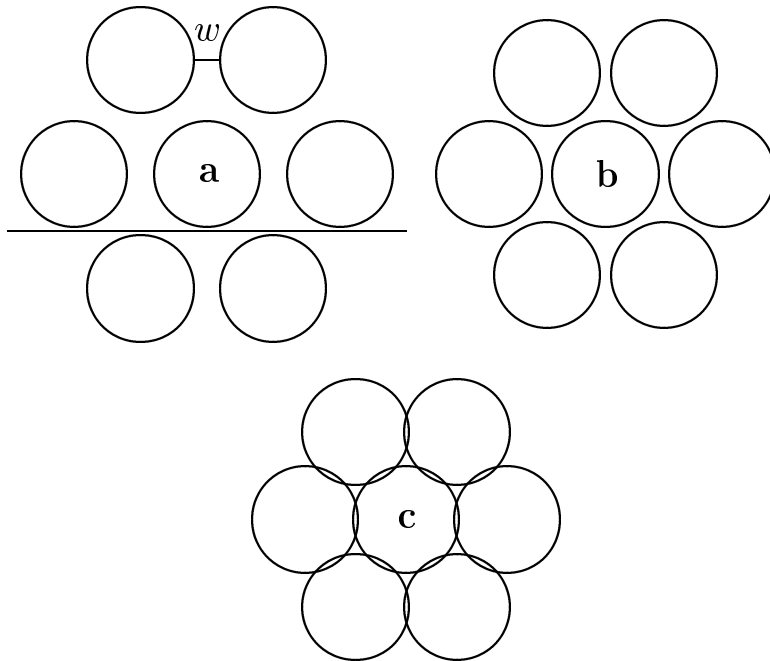


Figure 3: The periodic Lorentz gas with hexagonal lattice. The scatterers have unit radius. There are three regimes depending on the spacing  $w$ : (a) Infinite horizon,  $w > 4/\sqrt{3} - 2$ ; (b) Finite horizon,  $0 < w < 4/\sqrt{3} - 2$ ; (c) Overlapping,  $\sqrt{3} - 2 < w < 0$ .

section determined by the collisions, replacing the flow in continuous time by a map from one scatterer to the next, together with useful phase functions derived from the flow such as the time between collisions and the displacement between the centres of the initial and final scatterers. For the two dimensional Lorentz gas this corresponds to a two dimensional map, with the variables given by position on the scatterer and outgoing direction of the particle. For periodic models, the dynamics does not distinguish between scatterers due to translational invariance, but it is necessary to keep track of the displacement of the particle from its initial position in order to calculate, for example, the diffusion coefficient.

### 4.3 Green-Kubo relations

The method of Green [38] and Kubo [39] computes the linear transport coefficients in terms of time correlation functions of quantities computed in an equilibrium state. The relations can be derived either from linear response theory or an approach based on the Chapman-Enskog method of solving the Boltzmann equation (for example see Chap. 6 of Ref. [7]). Here we give a short derivation of the Green-Kubo relation for the diffusion coefficient, then discuss various extensions.

We begin by solving the diffusion equation for the probability density of finding a particle at a given position and time  $P(\mathbf{x}, t)$ , which is the Boltzmann distribution function  $f(\mathbf{x}, \mathbf{v}, t)$  integrated over velocity in the macroscopic limit (large times and distances),

$$\frac{\partial P}{\partial t} = D \nabla^2 P . \quad (32)$$

We used a Fourier transformed version of this equation to define the diffusion coefficient of the random Lorentz gas in Sec. 3.3. The equation is linear, so the general solution is an integral over the Green's functions given by the solution for an initial Dirac delta distribution  $P(\mathbf{x}, 0) = \delta(\mathbf{x} - \mathbf{x}_0)$ , that is,

$$P(\mathbf{x}, t) = (4\pi Dt)^{-d/2} \exp \left[ -\frac{(\mathbf{x} - \mathbf{x}_0)^2}{4Dt} \right] \quad (33)$$

where  $d$  is the spatial dimension. The mean square displacement of a particle is thus

$$\langle (\mathbf{x}_t - \mathbf{x}_0)^2 \rangle = \int (\mathbf{x} - \mathbf{x}_0)^2 P(\mathbf{x}, t) d\mathbf{x} = 2dDt \quad (34)$$

We expect the diffusion equation to approximate particle dynamics only at sufficiently large times, larger than typical correlation times since the diffusion equation contains no memory, and we have also neglected the velocity degrees of freedom. Thus we have

$$D = \lim_{t \rightarrow \infty} \frac{\langle (\mathbf{x}_t - \mathbf{x}_0)^2 \rangle}{2dt} \quad (35)$$

which is the Einstein relation for the diffusion coefficient. The diffusion coefficient is thus given (assuming the limit exists) by

$$\begin{aligned} D &= \frac{1}{2d} \lim_{t \rightarrow \infty} \frac{d}{dt} \langle (\mathbf{x}_t - \mathbf{x}_0)^2 \rangle \\ &= \frac{1}{d} \lim_{t \rightarrow \infty} \langle (\mathbf{x}_t - \mathbf{x}_0) \cdot \mathbf{v}_t \rangle \\ &= \frac{1}{d} \lim_{t \rightarrow \infty} \int_0^t \langle \mathbf{v}_{t'} \cdot \mathbf{v}_t \rangle dt' \\ &= \frac{1}{d} \int_0^\infty \langle \mathbf{v}_{t'} \cdot \mathbf{v}_0 \rangle dt' \end{aligned} \quad (36)$$

which is the Green-Kubo relation for diffusion. This relation has been used to calculate the diffusion coefficient of the periodic Lorentz gas [35].

A superdiffusive case where the mean square displacement grows faster than linearly with the time, such as when there is an infinite horizon, then corresponds to an infinite integral above, as when the velocity autocorrelation function decreases as  $1/t$  or slower with a finite number of sign changes. Systems that are subdiffusive with a slower growth of the mean square displacement correspond

to zero integral which is harder to observe, and not expected in the Lorentz gas unless a significant proportion of the disks are touching or overlapping.

Truncating the correlation integral at finite time gives (omitting the limits above) a time dependent diffusion coefficient, proportional to the time derivative of the mean square displacement at short times. Such a time dependent diffusion coefficient is useful to describe the “transient” response, that is, before correlations have died away.

Anisotropic systems can diffuse at different rates in different directions. The diffusion coefficient is replaced by a real symmetric positive definite matrix  $D_{ij}$ , which can then be diagonalised leading to  $d$  different coefficients along the coordinate axes. The symmetries of the Lorentz gas in a square or hexagonal lattice preclude such an anisotropic diffusion coefficient, however it occurs naturally with a rectangular lattice. As noted above, a rectangular lattice of one scatterer has an infinite horizon and hence anomalous diffusion, so at least two scatterers per unit cell are required to obtain anisotropic normal diffusion. Here we typically refer to the hexagonal Lorentz gas and write simply  $D$ , however it is easy to generalise most equations, for example (32,49) to the anisotropic case. Nonlinear response is more general, and leads to anisotropic behaviour even for the more symmetric hexagonal case (see Sec. 5.6).

A more general macroscopic equation for  $P(\mathbf{x}, t)$  would involve more spatial derivatives, corresponding to behaviour at shorter distances, and nonleading terms in the dispersion relation (14). The coefficients of such terms are called linear Burnett and super-Burnett coefficients (not to be confused with nonlinear Burnett coefficients involving higher powers of the forces). The time correlation function expressions for these coefficients [6] involve cumulants of the form

$$\langle v_0 v_t v_{t'} v_{t''} \rangle - \langle v_0 v_t \rangle \langle v_{t'} v_{t''} \rangle - \langle v_0 v_{t'} \rangle \langle v_t v_{t''} \rangle - \langle v_0 v_{t''} \rangle \langle v_t v_{t'} \rangle$$

integrated over all times. They are in general less convergent, so are expected to diverge for the random Lorentz gas due to its power law decay of correlations [20, 25]. This divergence corresponds to a nonanalytic dispersion relation (14), see Ref. [26]. The map corresponding to the finite horizon periodic Lorentz gas has exponential decay of correlations [40, 41], probably leading to convergence of all coefficients. See Ref. [6, 42] for the connection between this map and the diffusion and Burnett coefficients calculated in continuous time.

In general, all linear transport coefficients can be written in terms of integrals of time correlation functions similar to (36), with the velocity replaced by the relevant thermodynamic flux. For example, the viscosity is computed in terms of correlations of the shear stress, and thermal conductivity is computed in terms of correlations of the heat flux. All correlations are computed at equilibrium. Details can be found in Ref. [30].

There are a couple of limitations to the use of Green-Kubo relations for computing properties of nonequilibrium systems. The most obvious is that these relations apply only to linear response; they cannot be applied to systems far from equilibrium. The other limitation is that correlation functions being statistical in nature are difficult to calculate to a high degree of precision, compounded by the necessity of a numerical integration, often with a poor rate of

convergence. Both of these difficulties can be alleviated using thermostats, the subject of the next section.

## 5 Nonequilibrium molecular dynamics

### 5.1 Introduction to thermostats

A thermostat, as its name implies, is a device constructed to control the temperature. In the context of molecular dynamics simulations, it is a term added to the equations of motion of a system to simulate the effects of the environment. As such, thermostats serve two main purposes:

1. They allow simulation of nonequilibrium steady states. As noted in Sec. 2.1, nonequilibrium stationary states necessarily have contact with the environment. There are external forces and heat flows. In such situations a thermostat is needed to keep the energy of the system constant (either exactly or in an average sense), so that the system remains in a stationary state despite external forces that tend to increase the energy.
2. They allow simulation of different ensembles. Sec. 3.4 describes equilibrium ensembles in terms of contact with the environment, and also pairs of conjugate variables. The Nosé-Hoover thermostat (below) allows simulations in the canonical ensemble, by fixing the temperature and allowing the energy to vary. Similarly, thermostats may be designed to fix almost any system variable (for example kinetic energy, total energy, current, pressure, enthalpy) while leaving conjugate variables to vary. The various thermostats can thus be understood as the ensembles of nonequilibrium statistical mechanics. It is expected that they should lead to equivalent results in the thermodynamic limit (except for fluctuations in the fixed quantities) as do the equilibrium ensembles, at least in the linear regime [30, 43, 44].

An alternative to a thermostat where environmental effects are put in the equations of motion is to simulate such effects at the boundary, which we discuss in Sec. 6; an advantage of thermostats is that they permit the simulation to remain homogeneous, see Sec. 4.1.

A common objection to the use of thermostats is that they add “unphysical” forces to Newtons “exact” equations of motion. The fact is that any scheme used to replace an unbounded environment by a finite number of degrees of freedom (including alternative boundary methods) must unavoidably make drastic approximations. Some facts that inspire confidence in thermostatted methods are their ensemble equivalence (above) and their agreement with Green-Kubo relations for linear transport coefficients. Far from equilibrium, thermostatted approaches should apply whenever the bulk of the system is in contact with the environment, either because it is two dimensional, or thermal transfer by radiation is sufficiently strong.

## 5.2 Gaussian and Nosé-Hoover thermostats

A simple method of ensuring that a nonequilibrium molecular dynamics simulation remains stationary in time despite external forcing is to periodically renormalise the velocities of all the particles to keep the (kinetic or internal) energy constant. If the time interval between successive renormalisations is reduced to zero, we obtain the Gaussian thermostat, discovered independently for the kinetic energy by Hoover and collaborators [45] and for the internal energy by Evans [46]:

$$\begin{aligned}\dot{\mathbf{x}} &= \mathbf{p} \\ \dot{\mathbf{p}} &= \mathbf{F}_i + \mathbf{F}_e - \alpha \mathbf{p}\end{aligned}\tag{37}$$

Here the mass  $m = 1$  and the particle indices have been suppressed, leading to a description in terms of  $Nd$ -dimensional vectors.  $\mathbf{F}_i$  contains all the interparticle forces as described in Sec. 4.1,  $\mathbf{F}_e$  contains external driving forces, and  $\alpha$  is a scalar thermostat “friction coefficient” which is the same for all particles and directions.

The value of  $\alpha$  is determined by the desired constraint: For constant kinetic energy we have the Gaussian isokinetic thermostat,

$$\alpha_{GIK} = \frac{(\mathbf{F}_i + \mathbf{F}_e) \cdot \mathbf{p}}{\mathbf{p} \cdot \mathbf{p}}\tag{38}$$

where the dot product includes a sum over the particles. It is easily verified that the kinetic energy  $K = \mathbf{p} \cdot \mathbf{p}/2$  is identically preserved by these equations. The term “Gaussian” applies to Gauss’ principle of least constraint, whereby these equations may be derived by demanding the smallest constraint force (according to the above dot product) at any time, see [30, 47].

For constant internal (kinetic plus interparticle) energy we have the Gaussian isoenergetic thermostat,

$$\alpha_{GIE} = \frac{\mathbf{F}_e \cdot \mathbf{p}}{\mathbf{p} \cdot \mathbf{p}}\tag{39}$$

which preserves  $K + \phi_i$  assuming that the internal forces are conservative,  $\mathbf{F}_i = -\nabla \phi_i$ .

In this notation the Nosé-Hoover approach treats the thermostating multiplier  $\alpha$  as an additional dynamical variable with a feedback mechanism, so we have for the Nosé-Hoover (isokinetic) thermostat

$$\dot{\alpha}_{NHIK} = \frac{2}{Q}(K - K_0)\tag{40}$$

where  $Q$  is a constant that determines the time scale of the feedback and  $K_0$  is the desired kinetic energy, usually  $Ndk_B T/2$ . This is (apart from slight differences in notation) Hoover’s reformulation of the Nosé thermostat discussed in Sec. 5.4, see Refs. [48, 49, 50]. The feedback operates as follows: Suppose the initial kinetic energy becomes too high, then  $\dot{\alpha}$  is positive, leading to more

damping in (37) which then decreases the kinetic energy, and similarly if the kinetic energy becomes too small. It is also possible to replace the  $K$ 's above by the internal energy to construct a Nosé-Hoover isoenergetic thermostat.

All of these thermostats simulate the exchange of thermal energy between the system and its environment. On the average this flow is outward (zero at equilibrium), corresponding to positive  $\langle\alpha\rangle$ , however there is no reason that  $\alpha$  should not become negative occasionally, unlike macroscopic frictional forces. To be more precise, we can compute the amount of heat being removed by the thermostat and use irreversible thermodynamics (Sec. 2) to write

$$\dot{S}_{irr} = \alpha \frac{\mathbf{P}^2}{T} \quad (41)$$

from which we deduce that the non-negativity of  $\alpha$  on average is guaranteed by the second law.

In the limit of large systems, we expect that all the various processes that the particles undergo tend to average out, leading to a more or less constant value of  $\alpha$ , as well as various macroscopic variables[51]. This is consistent with the very low probability of a decrease in entropy in a large dissipative system. Because the fluctuations of all thermodynamic quantities are smaller in large systems (except near phase transitions), different thermostats approach the same thermodynamic state, another statement of ensemble equivalence.

At equilibrium, that is, with no external force  $\mathbf{F}_e$  it is clear that the isoenergetic thermostat multiplier  $\alpha_{IE}$  is identically zero, while the other thermostats vary around zero. The Nosé-Hoover thermostat is special in that the equations generate the canonical ensemble [48, 49, 50], that is, assuming the dynamics is ergodic (a reasonable assumption in practice for all but the smallest systems based on numerical work [52]), the probability distribution of  $\mathbf{x}$  and  $\mathbf{p}$  (averaging over  $\alpha$ ) is given by (19). This means that the Nosé-Hoover thermostat can be (and is) used to simulate an equilibrium system at fixed temperature, rather than fixed energy.

There are many other types and uses of thermostats. There are specific algorithms for computing all possible transport coefficients. For example, shear viscosity can be computed using “sliding brick” boundary conditions, thermostatted such that the temperature is measured relative to a linear velocity profile characteristic of Couette flow. Thermal conductivity can be computed by including forces that accelerate hot and cold particles in different directions. Both of these examples are homogeneous, with no dependence of distributions on position. There are also inhomogeneous algorithms, where different parts of a system (for example particles sufficiently close or belonging to the walls) are thermostatted at different temperatures, or at the same temperature relative to different velocities. Finally, it is possible to apply thermostats to enforce other ensembles, for example constant pressure (hence fluctuating volume). All these examples and more are described in texts on nonequilibrium molecular dynamics [29, 30, 31]. A more recent review of the Gaussian and Nosé-Hoover thermostats with a discussion of Gauss’ principle and application to the Lorentz gas is given in Ref. [47].

### 5.3 The nonequilibrium Lorentz gas

Just as the random Lorentz gas appears as one of the simplest applications of the Boltzmann equation (Sec. 3.3) and the periodic Lorentz gas appears as one of the simplest examples of equilibrium molecular dynamics (Sec. 4.2), so the (more precisely “a”) nonequilibrium Lorentz gas appears as one of the simplest examples of nonequilibrium molecular dynamics. We begin with a description of the “colour diffusion” algorithm for the self diffusion coefficient, see Ref. [30]. This is arguably the simplest nonequilibrium molecular dynamics algorithm, as it is homogeneous, involves only the usual periodic boundary conditions, and the external force on each particle is a constant.

The self diffusion coefficient is the limit of the mutual diffusion coefficient of a mixture of two species that become identical. In the colour diffusion algorithm, each particle is assigned a positive or negative “colour charge” which (unlike electric charge) has no effect on the interparticle forces, but determines the interaction with an external “colour field”  $\mathbf{E}_c$ . Thus the external force on particle  $i$  with charge  $c_i$  is  $\mathbf{F}_e = c_i \mathbf{E}_c$ . The response to such an external field is the “colour current”,  $\mathbf{J}_c = \sum c_i \mathbf{p}_i / m$ . The diffusion coefficient (equivalent to “colour conductivity”) is then proportional to the ratio  $|\langle \mathbf{J}_c \rangle| / |\mathbf{E}_c|$  in the limit  $|\mathbf{E}_c| \rightarrow 0$ . In order for the time average of the current to make sense, a thermostat must be applied. From the point of view of calculating the linear response of a many particle system, it doesn’t matter which thermostat is applied, or whether it is applied to the whole system or to the two types of particles separately.

The simplest such case of the colour diffusion algorithm is thus two particles (one of each colour charge) interacting with a hard ball potential in two dimensions with a Gaussian thermostat (since a Nosé-Hoover thermostat has an extra phase space variable  $\alpha$ ). The isokinetic and isoenergetic thermostats are equivalent here, since the internal force is zero outside collisions, and the collisions are not affected by either thermostat. As in Sec. 4.2 we consider relative coordinates, which reduces the problem to that of a single point particle moving in a periodic cell under the influence of a constant field  $\mathbf{F}$  and a thermostat, and colliding with a single circular scatterer: The nonequilibrium Lorentz gas [53].

The thermostat ensures that twice the energy of the particle,  $\mathbf{p}^2/m$  is constant, so as before it is possible to set the magnitude of the momentum, the mass and the radius of the scatterer equal to unity by appropriate scaling. The equations of motion are thus

$$\dot{\mathbf{x}} = \mathbf{p} \tag{42}$$

$$\dot{\mathbf{p}} = \mathbf{F} - \mathbf{F} \cdot \mathbf{p} \mathbf{p} \tag{43}$$

Note that the denominator of (38) for  $\alpha_{GIK}$  may be set equal to unity due to the constancy of the kinetic energy, so that the equations for the nonequilibrium Lorentz gas, generalised to arbitrary dimension and position dependent external forces apply to many particle systems constrained by the Gaussian isokinetic thermostat, and hence approximately to other thermostatted systems

when ensemble equivalence holds. This close connection between the nonequilibrium Lorentz gas and many particle systems in a nonequilibrium steady state is extremely useful in discovering and demonstrating general properties of the latter.

The solution of the isokinetic equations for the Lorentz gas is most easily expressed in terms of the angle  $\theta$  between the direction of motion and the field, which is assumed to be in the positive  $x$  direction and have magnitude  $F$ . Specifically  $p_x = \cos \theta$  and  $p_y = \sin \theta$  in two dimensions, leading to  $\dot{\theta} = -F \sin \theta$ . Given initial conditions with a subscript 0, the solutions are

$$\tan(\theta/2) = \tan(\theta_0/2) \exp\left(-\frac{t-t_0}{F}\right) \quad (44)$$

$$x = x_0 - \frac{1}{F} \ln\left(\frac{\sin \theta}{\sin \theta_0}\right) \quad (45)$$

$$y = y_0 - \left(\frac{\theta - \theta_0}{F}\right) \quad (46)$$

with direct generalisations to higher dimensions. Note that the displacement transverse to the field  $y - y_0$  cannot exceed  $\pi/F$ ; the particle rapidly approaches the direction of the field. The transcendental functions make it difficult to determine analytically when a collision with the circular scatterers takes place; one possible numerical approach is to put a lower bound on the time to the next collision using a circular approximation to the trajectory, moving forward this time step, and iterating to convergence [54]. In spite of this difficulty, it is possible to obtain analytic expressions for the linear integrated equations used to compute the Lyapunov exponents in terms of the initial and final angles of each free path between collisions, see Refs. [47, 55].

In response to the external field  $\mathbf{F}$  and collisions with the (usually hexagonal) lattice the particle drifts with a current given by

$$\mathbf{J} = \dot{\mathbf{x}} \quad (47)$$

assuming finite horizon. Using Eq. (38) with  $|\mathbf{p}| = 1$  for  $\alpha$  we find

$$\mathbf{J} \cdot \mathbf{F} = \alpha \quad (48)$$

in agreement with (41). In the limit of small field the average current is the same for almost all (Lebesgue) initial conditions [57] and is given by

$$\langle \mathbf{J} \rangle = D\mathbf{F} + o(\mathbf{F}) \quad (49)$$

where  $D$  is the diffusion coefficient, or tensor in the anisotropic case. For the case of infinite horizon, there are two possibilities: When the field is along one of the infinite horizon directions the particle almost always ends up moving without collisions along this direction, otherwise the current appears normal. The zero field limit is thus not defined, and in any case would correspond to anomalous diffusion.

The equations of motion of the nonequilibrium Lorentz gas have the following immediate properties, which also apply to more general thermostatted systems:

1. Time reversibility: Reversing the direction of time is equivalent to replacing  $\mathbf{p}$  by  $-\mathbf{p}$ , as in Newtonian (unthermostatted) mechanics. This has the effect of changing the sign of  $\alpha$ . On the Poincaré section determined by the surface of the scatterers this corresponds to a reflection in the outgoing angle across the normal to the scatterer, that is, replacing  $\theta$  by  $\theta + 2\chi$  in Fig 1.
2. Phase space contraction: Liouville's equation (21) implies that the rate of growth of a volume element  $\delta V$ , which is inversely proportional to the probability density  $\rho$  evolves according to

$$\frac{\delta \dot{V}}{\delta V} = -\frac{1}{\rho} \frac{d\rho}{dt} = -\frac{1}{\rho} \left( \frac{\partial \rho}{\partial t} + F \cdot \nabla \rho \right) = \nabla \cdot F \quad (50)$$

Evaluating  $\nabla \cdot F$  for the equations of motion, (37) with (38-40) we find

$$\nabla \cdot F = \begin{cases} -(Nd-1)\alpha_{GIK} \\ -(Nd-1)\alpha_{GIE} \\ -Nd\alpha_{NHIK} \end{cases} \quad (51)$$

which reduces to  $-\alpha$  in the two dimensional Lorentz gas. The collisions of the Lorentz gas (or other hard ball systems) are instantaneous and preserve phase space volume, so they do not affect the above formulae.

The phase space contraction has a number of effects, namely that the sum of the Lyapunov exponents is negative, and related to the average value of  $\alpha$ ,

$$\sum \lambda = \langle \nabla \cdot F \rangle \quad (52)$$

For the case of the two dimensional Lorentz gas, the Kaplan-Yorke relation gives the information dimension [56] of the attractor for the Poincaré map for sufficiently small field [57],

$$D_1 = 1 + \frac{\lambda_1}{|\lambda_2|} = \frac{2\lambda_1 + \langle \alpha \rangle}{\lambda_1 + \langle \alpha \rangle} \quad (53)$$

This is less than the dimension of the map (two) since the phase space contraction requires the density to concentrate on a small set most of the time. Nevertheless, the attractor is dense in phase space for sufficiently small field [57],

$$D_0 = 2 \quad (54)$$

Numerical evidence for what “sufficiently small” implies in practice is given below, Sec. 5.6. The concentration of the density onto multifractal distributions means that for the steady state, the density becomes a distribution, and is studied by means of more general techniques, such as Sinai-Ruelle-Bowen (SRB) measures or periodic orbit measures, Sec. 5.5.

It is clear from Eq. (41) that  $\alpha$  is related to the rate of entropy production, so now phase space contraction can also be related to entropy production. The

Gibbs entropy, Sec. 3.4, which was constant for equilibrium (specifically phase space volume conserving) systems, now decreases to negative infinity!

$$\lim_{t \rightarrow \infty} \frac{dS_G}{dt} = \lim_{t \rightarrow \infty} \int (\nabla \cdot F) \rho d\Gamma = -\langle \alpha \rangle < 0 \quad (55)$$

Needless to say, this has been the source of a large amount of confusion in the literature. The correct resolution is probably along the following lines: The Gibbs entropy is telling us (appropriately) that entropy is being removed from the system via the thermostat; it does not take into account irreversible entropy production in the system, as it did not do so for isolated systems; it cannot tell us about the entropy increase in the environment since the phase space does not include these degrees of freedom. There have been a number of attempts (mostly in connection with Baker maps) to coarse grain the Gibbs entropy of a nonequilibrium system, in order to take into account the irreversible entropy production. This is a very active area of discussion at present, see Refs. [10, 28].

The accumulated phase space contraction along a trajectory is easily found to be

$$\frac{\delta V(t)}{\delta V(0)} = e^{-\int_0^t \alpha(t') dt'} \quad (56)$$

for the nonequilibrium Lorentz gas (with obvious extensions to all the thermostats considered above), corresponding to a probability density of

$$\frac{\rho(\mathbf{x}_t, t)}{\rho(\mathbf{x}_0, 0)} = e^{\int_0^t \alpha(t') dt'} \quad (57)$$

assuming continuous distributions. This is an example of a Kawasaki distribution function [30, 58]. The argument of the exponential gives the total amount of entropy removed by the thermostat; for the Lorentz gas this is

$$\int_0^t \alpha(t') dt' = \int_0^t \mathbf{J} \cdot \mathbf{F} dt' = \int \mathbf{F} \cdot d\mathbf{x} = -\Delta \Phi \quad (58)$$

assuming the external force is conservative,

$$\mathbf{F} = -\nabla \Phi \quad (59)$$

For the Lorentz gas,  $\Phi$  is a linear function of the coordinates. This expression for the accumulated phase space contraction provides a motivation for the symplectic structure of the next section, as well as a basis for a discussion of time reversibility.

Newton's equations are time reversible, so one of the difficulties in understanding the second law of thermodynamics is that for any system observed to increase in entropy, it is possible to set up a time reversed system with a decrease in entropy with time. Boltzmann's solution (Sec. 3.1, Ref. [12]) is that the most likely states (corresponding to large regions of phase space) are those with high entropy; the initial state of the Universe has very low entropy for some reason, but the final state is not constrained in this way. In the same way, for every

trajectory in a thermostatted system with positive  $\alpha$  and hence positive entropy production, there is a time reversed trajectory with the opposite. However a uniform initial distribution, or in fact any smooth initial distribution, has (at long times) a greater probability of positive  $\alpha$  leading to a positive  $\langle\alpha\rangle$ . This is because the volume in phase space is bounded, and so only an exponentially small proportion of trajectories can grow with a positive exponential, while the remainder are forced to contract to make room for the growing trajectories. A more quantitative description can be given in terms of periodic orbits, see Sec. 5.5 and Ref. [59].

If, in addition to phase space contraction, sufficiently strong chaotic properties (“Anosov-like”) can be assumed, the ratio of the probabilities that a trajectory of length  $\tau$  will have entropy production  $\Delta S$  (as measured by the phase space contraction above) or  $-\Delta S$  in the limit  $\tau \rightarrow \infty$  approaches  $e^{\Delta S}$ . The limit is taken keeping the entropy production rate  $\Delta S/\tau$  constant. This result, called the fluctuation theorem was first observed for shearing flow in Ref. [60] and proved in Refs. [61, 62]. It applies to the Lorentz gas if the field is not too large; although it is not strictly Anosov due to the collisions, it nevertheless retains very strong chaotic properties. The fluctuation theorem and its generalisations are an active area of investigation at present [9].

#### 5.4 Symplectic properties

Another of the unexpected properties of thermostatted systems (in particular those with isokinetic thermostats) is that, despite phase space contraction, it is possible to express the dynamics in terms of Hamiltonian equations which are by definition (23) phase space conserving. The first such formulation was the original Nosé thermostat [48, 49, 50],

$$H_N(\mathbf{x}, s; \boldsymbol{\pi}, p_s; \lambda) = \sum_{i=1}^N \frac{|\boldsymbol{\pi}_i|^2}{2m_i s^2} + \phi(\mathbf{x}) + \frac{p_s^2}{2Q} + 2K_0 \ln s \quad (60)$$

Here  $s$  and its conjugate momentum  $p_s$  are supposed to represent the “heat bath”. If we interpret the time variable  $\lambda$  as related to physical time  $t$  by  $dt = d\lambda/s$  then we can derive Hoover’s form of the equations, Eqs. (37,40) using  $\mathbf{p}_i = m_i d\mathbf{x}_i/dt = \boldsymbol{\pi}_i/s$  and  $\alpha = p_s/Q$  (and in our case, setting the masses equal to one). Note that rewriting the equations in this manner has reduced the number of dimensions of phase space by one, since the equations of motion for  $\mathbf{x}$ ,  $\mathbf{p}$  and  $\alpha$  do not contain  $s$ . This also means that there is no manifest constant of motion (given by  $H_N$ ) for the new form of the equations. The new equations are phase space contracting because they are written in different variables — the physical momentum  $\mathbf{p}$  differs from canonical momentum  $\boldsymbol{\pi}$  by a factor  $s$ , which keeps track of the entropy production since its equation of motion is  $ds/dt = \alpha s$ .

Another Hamiltonian for a thermostatted system is that of the Gaussian isokinetic thermostat, which in contrast to the Nosé-Hoover thermostat has a manifest constant of motion, namely the kinetic energy. Thus it is natural for the Hamiltonian to be some function of the kinetic energy, written so that the

physical and canonical momenta vary by the accumulated phase space contraction,  $e^{\Delta\Phi}$  (see the end of the previous section). In fact, the Hamiltonian [16]

$$H_G(\mathbf{x}; \boldsymbol{\pi}; \lambda) = e^{2\Phi} \frac{\boldsymbol{\pi}^2}{2} \quad (61)$$

with the interpretation  $dt = e^\Phi d\lambda$  leads to the Gaussian isokinetic equations (37,38) with  $\mathbf{p} = e^\Phi \boldsymbol{\pi}$  and  $\mathbf{F} = -\nabla\Phi$  when the constraint  $\mathbf{p}^2 = 1$  is imposed. This is also a Hamiltonian that generates geodesics [63] on the space with conformally flat metric

$$ds^2 = e^{-2\Phi} d\mathbf{q}^2 \quad (62)$$

leading to variational approaches based on finding the stationary (usually minimum) geodesic length, and an interpretation as light passing through a medium with refractive index  $n = e^{-\Phi}$ .

There is a third thermostat with a Hamiltonian description, namely the isoenergetic thermostat (39) restricted to the case where the internal and external forces are proportional, that is  $\mathbf{F}_e = -\gamma\mathbf{F}$ ,  $\mathbf{F}_i = (1 - \gamma)\mathbf{F}$  with  $\gamma$  constant and  $\mathbf{F} = -\nabla\Phi$ . The momentum equation is then

$$\frac{d\mathbf{p}}{dt} = \mathbf{F} - \gamma \frac{\mathbf{F} \cdot \mathbf{p}}{\mathbf{p}^2} \mathbf{p} \quad (63)$$

with the conserved energy  $E_\gamma = \mathbf{p}^2/2 + (1 - \gamma)\Phi$ . This restricted isoenergetic thermostat is not realistic from the point of view of internal and external forces being proportional; rather it allows a continuous interpolation between the case of no thermostat  $\gamma = 0$  to that of the isokinetic thermostat  $\gamma = 1$ . Because the kinetic energy is no longer constant, the denominator cannot be ignored, in fact an additive constant is added to  $\Phi$  to ensure that  $E_\gamma$  is zero, then  $\mathbf{p}^2$  can be replaced by  $-2(1 - \gamma)\Phi$ . Noting that  $\mathbf{F}/\Phi$  can be written  $-\nabla \ln |\Phi|$ , the accumulated phase space contraction (56) is thus  $|\Phi|^{\gamma/(2(1-\gamma))}$ . Paralleling the isokinetic thermostat, we then arrive at the “restricted Gaussian isoenergetic” Hamiltonian [64]

$$H_{RGIE}(\mathbf{x}; \boldsymbol{\pi}; \lambda) = |\Phi|^{-\gamma/(1-\gamma)} \frac{\boldsymbol{\pi}^2}{2} + (1 - \gamma)\Phi \quad (64)$$

which, coupled with the constraint  $H_{RGIE} = 0$  and the time scaling  $dt = |\Phi|^{-\gamma/(2(1-\gamma))} d\lambda$  leads to the above equations of motion.

It was noted in [16] for the Gaussian isokinetic thermostat, in [65] for the Nosé-Hoover thermostat, and in [64] for the restricted Gaussian isoenergetic thermostat that the somewhat arbitrary time scaling may be obviated by adding a constant to the Hamiltonian to make its numerical value zero, and then multiplying by an appropriate factor, namely  $e^{-\Phi}$  for the Gaussian thermostat and  $s$  for the Nosé-Hoover thermostat. In general, the Gaussian isokinetic Hamiltonian with a time scaling of  $dt = e^{\beta\Phi} d\lambda$  becomes

$$H_\beta(\mathbf{x}; \boldsymbol{\pi}; \lambda) = e^{(\beta+1)\Phi} \frac{\boldsymbol{\pi}^2}{2} - \frac{e^{(\beta-1)\Phi}}{2} \quad (65)$$

with the isokinetic constraint simply  $H_\beta = 0$ . These Hamiltonians apply to thermostatted systems with arbitrary conservative forces and arbitrary numbers of particles. The Lorentz gas version of the case  $\beta = -1$  corresponding to the familiar kinetic plus potential energy Hamiltonian was noted by Hoover and collaborators eight years previously [66].

The Hamiltonian gives an alternative derivation of the solutions of the equations of motion of the nonequilibrium Lorentz gas, Eqs. (44-46). The potential  $\Phi = -Fx$  does not depend on  $y$ , so  $\pi_y = e^{Fx} p_y$  is a constant of the motion.  $p_x$  is determined by the constraint  $p_x^2 + p_y^2 = 1$ , allowing an immediate solution in cartesian coordinates by integration.

While the equations of motion of these thermostats can be derived from a Hamiltonian, the global structure including the periodic boundary conditions is not strictly Hamiltonian. This is because the potential  $\Phi$  (for example) is not periodic; for the Lorentz gas it is a linear function of position. The lack of a global Hamiltonian allows the steady state distributions not to be uniform on some energy surface; they are typically multifractal. In spite of this, the local symplectic structure is sufficient to ensure the pairing of Lyapunov exponents, discussed next. The isokinetic Hamiltonian has also been applied to a definition of temperature using the Boltzmann entropy in [15]. Choquard [67] has a further exposition of the variational properties of the isokinetic thermostat, including a Lagrangian approach and a link with the conformally symplectic formalism used in Ref. [68] for a proof of the pairing rule, below.

We have already seen the Lyapunov sum rule (52), which relates the entropy production, a macroscopic quantity, to the sum of the Lyapunov exponents, a microscopic quantity. The pairing of Lyapunov exponents, also called the conjugate pairing rule or symmetry of the Lyapunov spectrum, is a much stronger property, relating individual pairs of Lyapunov exponents. It is proved using the symplectic property of the dynamics, and appears to be limited in validity to systems admitting a Hamiltonian description.

It has been known for some time that the Lyapunov exponents of a Hamiltonian system come in  $\pm$  pairs, that is, they may be split into groups of two, each of which sums to zero [69]. In 1988 Dressler [70] showed that for a constant frictional coefficient  $\alpha$ , the sum of each pair of Lyapunov exponents is  $-\alpha$ . Incidentally, the constant  $\alpha$  “thermostat” can also be derived from a Hamiltonian, obtained as for the isokinetic thermostat above, with the accumulated phase space contraction  $e^\Phi$  replaced by  $e^{-\alpha t} = 1/(\alpha\lambda)$ . In contrast to the usual thermostats, this Hamiltonian is explicitly time dependent.

Meanwhile, numerical simulations of many particle systems where Lyapunov exponents were computed began to show evidence for a similar law [30, 71, 72, 73]. Ironically the first observations of Lyapunov exponent pairing were in shearing systems, where more detailed recent computations have ruled out exact pairing [74]. Initially the results were explained in terms of the large number of particles [75]. In systems of many particles it is often easier to compute the largest and smallest Lyapunov exponents than the whole spectrum, so the pairing rule if it holds can be used to relate these measurable exponents to the entropy production and (also measurable) transport coefficients.

In order to clarify the role of the system size, and also because it is possible to compute Lyapunov exponents more precisely in small systems, the author and two collaborators studied the Lyapunov exponents of the simplest thermostatted system with more than one nontrivial pair of Lyapunov exponents, the three dimensional Lorentz gas [54]. The results, that two pairs of Lyapunov exponents each sum to  $-\langle\alpha\rangle$  whether positive or negative and that a trivial pair is zero due to the conservation of kinetic energy, were extremely helpful in understanding the conditions under which pairing occurs. In this case at least, pairing does not depend on a large system limit, or on chaotic properties associated with positive Lyapunov exponents, so it must be derived from the equations of motion. The degrees of freedom corresponding to the direction of the flow and the conserved kinetic energy give zero exponents not summing to  $-\langle\alpha\rangle$ , so they must somehow be excluded from consideration. With these points in mind, we move on to a statement of the result and a sketch of the proof.

The conjugate pairing theorem states that for the isokinetic thermostat and the restricted isoenergetic thermostat discussed above there are two zero Lyapunov exponents, and the remaining  $Nd-1$  pairs of exponents sum to  $-\langle\alpha\rangle-\lambda$ . The Nosé-Hoover thermostat is the same except that there is one zero exponent and  $Nd$  pairs. The Lyapunov exponents and average values of  $\alpha$  are computed using the same invariant measure, which may be any trajectory or invariant measure of the system. In particular, the theorem holds irrespective of chaotic properties such as ergodicity or positive Lyapunov exponents, and irrespective of the size of the system.

The main ideas of the proof are sketched below; details can be found for the isokinetic thermostat in Refs. [68, 76, 77], the restricted isoenergetic thermostat in Ref. [78] and the Nosé-Hoover thermostat in Refs. [65, 68]. Refs. [68, 77] explicitly include the collisions, and the isokinetic thermostat on a curved manifold. Numerical evidence excludes pairing in shearing systems [74] and a more general isoenergetic thermostat [78].

Hamiltonian dynamics can be written most simply using a matrix

$$J = \begin{pmatrix} 0 & I \\ -I & 0 \end{pmatrix} \quad (66)$$

where  $I$  is the unit submatrix, and the block form corresponds to  $\mathbf{x}, \boldsymbol{\pi}$ . We have the transpose  $J^T = -J$  and  $J^2 = -1$ . Then Hamilton's equations are  $\dot{\Gamma} = J\nabla H$  and the equation of motion for perturbations is  $\delta\dot{\Gamma} = T(t)\delta\Gamma$  where  $T = J\nabla\nabla H$ . The matrix  $T$  satisfies the equation  $T^T J + JT = 0$  (where a superscript  $T$  denotes transpose) due to derivatives of  $H$  commuting, compare with Liouville's theorem (23). The first step to prove the pairing rule is to show that the appropriate matrix  $T$  satisfies a generalised equation,

$$T^T J + JT = -\alpha J \quad (67)$$

For the case of constant  $\alpha$  this is straightforward, but for the other thermostats it is first necessary to reduce the space to exclude the zero exponents by ruling out perturbations that are parallel to the flow, and for the isokinetic thermostat,

those that violate the constant energy condition. The  $T$  matrix then contains coefficients of the constrained perturbation equations. Refs. [68, 77] also prove an equivalent condition for the hard collisions.

The equation (67) for the perturbation evolution equations can be extended to finite evolutions  $\delta\Gamma(t) = L(t)\delta\Gamma(0)$  using the equation for the  $L$  matrix,  $\dot{L} = TL$  with initial condition  $L(t=0) = 1$  to obtain

$$\mu L^T J L = J \tag{68}$$

where  $\mu = \exp(\int_0^t \alpha dt)$ . Consider the eigenvalues of  $M = L^T L$ , which obeys  $\mu^2 M^T J M = J$  following from (68). Straightforward matrix manipulations of the eigenvalue equation leads to the result that the eigenspace of an eigenvalue  $\Lambda^2$  is transformed by  $J$  into an eigenspace with eigenvalue  $1/(\Lambda^2 \mu^2)$ . The Lyapunov exponents are the infinite time limit of the logarithm of the eigenvalues, divided by twice the time. Thus the spectrum is symmetric with the pairs summing to  $-\langle\alpha\rangle$ , and the theorem is proved.

## 5.5 Periodic orbit approaches

It was noted in Sec. 5.3 above that invariant measures of thermostatted nonequilibrium systems (including the Lorentz gas) are multifractal. This means in particular that the concept of a smooth probability density  $\rho(\Gamma)$  must be replaced by a more general description.

The most primitive approach is to coarse grain the space into arbitrary partitions (say, of equal size) and count the number of times a long (hopefully typical) trajectory passes through each cell. This does not depend on strong chaotic properties; ergodicity is sufficient to define a unique measure. The disadvantages are that there are few mathematical results for such a general framework, the partition does not take into account the natural structure of the dynamics, and it is not immediately clear how to define measures on repellers of open systems, which almost all trajectories leave after a finite (typically rather short) time, see Sec. 6.

It may be possible to prove (or make a plausible hypothesis) that the dynamics is sufficiently hyperbolic that there are invariant measures smooth along unstable (expanding) directions in phase space; these are called Sinai-Ruelle-Bowen (SRB) measures. While it is possible to prove a number of results pertaining to such systems [32, 77], a proof of the existence of (for example) a Markov partition does not necessarily show how to construct it efficiently, and is of no use if the required dynamical properties have not been shown. For the nonequilibrium Lorentz gas, rigorous results are mostly restricted to the case of small field and finite horizon, see for example [57].

Periodic orbit theory [3, 79] provides both the mathematical justification (given sufficiently strong hyperbolicity [80]) and also gives explicit expressions for multifractal measures that can be applied to many systems (with apparent success, although sometimes slower convergence [81]) for which enough periodic orbits can be located, but rigorous proofs are not available. In addition, the

periodic orbits are coordinate invariant, make use of the dynamics in a natural manner, and are applicable to open systems. We refer here to classical periodic orbit theory; there are similar theories applicable to quantum systems in the semiclassical limit [3, 82] and more recently to stochastically perturbed classical systems [83, 84].

It may seem strange that the properties of a system can be determined from a set of zero measure orbits such as the periodic orbits; to make an analogy, numerical integration schemes often use only rational points at which to evaluate the integrand. The main question is whether the set of zero measure (rational points or periodic orbits) is dense in the measure (phase space or some lower dimensional attractor). For the case of periodic orbits, this is usually either proven or a reasonable assumption.

Periodic orbits arise naturally when system properties are computed from the spectrum of evolution operators. The desired property is first expressed in terms of a generating function that is multiplicative in time, for example the current (for the nonequilibrium case) and the diffusion coefficient (for the equilibrium case) are expressed as

$$J_i = \frac{\partial}{\partial \beta_i} s(\boldsymbol{\beta})|_{\boldsymbol{\beta}=0} \quad (69)$$

$$D = \frac{1}{d} \text{tr} D_{ij} = \frac{1}{2d} \sum_i \frac{\partial}{\partial \beta_i} \frac{\partial}{\partial \beta_i} s(\boldsymbol{\beta})|_{\boldsymbol{\beta}=0} \quad (70)$$

$$s(\boldsymbol{\beta}) = \lim_{t \rightarrow \infty} \frac{1}{t} \ln \langle e^{\boldsymbol{\beta} \cdot \Delta \mathbf{x}} \rangle \quad (71)$$

using the Einstein relation (35) where  $\boldsymbol{\beta}$  is a dummy variable,  $\Delta \mathbf{x} = \mathbf{x}(t) - \mathbf{x}(0)$  and  $s(\boldsymbol{\beta})$  gives the rate of exponential growth of the average, and is thus the leading eigenvalue of the Liouville operator weighted by the exponential.

The leading eigenvalue of an evolution operator (such as a weighted Liouville operator) may be computed in a number of ways. Some of the most common, namely the long time asymptotic form of its trace, Ruelle's dynamical zeta function, and the Fredholm determinant lead to expressions in terms of periodic orbits [3, 4, 7, 79, 85]. For example the most rapidly convergent expressions usually come from the Fredholm determinant of a discrete time system (for example using the collisions of the Lorentz gas to define the dynamics),  $\det(1 - z\mathcal{L})$  where  $z = e^{-s}$  and  $\mathcal{L}$  is the weighted evolution operator. The determinant is then expanded using the general matrix relation  $\det M = e^{\text{tr} \ln M}$  to a maximum order in  $z$ . The resulting expression involves  $\text{tr} \mathcal{L}^n$  which counts the ways the system can return to its starting point after  $n$  iterations, the periodic orbits of length  $n$ . Specifically,

$$\text{tr} \mathcal{L}^n = \sum_{\mathbf{x}: \mathbf{f}^n(\mathbf{x}) = \mathbf{x}} \frac{e^{\boldsymbol{\beta} \cdot \Delta \mathbf{x}}}{|\det(1 - J^{(n)}(\mathbf{x}))|} \quad (72)$$

where  $J$  is the Jacobian matrix of derivatives of  $\mathbf{f}^n$ , the  $n$ th iterated Poincaré map.

The denominator is often approximated by  $|\Lambda|$ , the product of the expanding eigenvalues of  $J$ , that is, those with a magnitude strictly greater than one.  $|\Lambda|$  is also given by  $e^T \sum \lambda_+$ , the exponential of the period times the sum of the positive Lyapunov exponents along the periodic orbit. Approximating the denominator of (72) by  $|\Lambda|$  is exact in the limit of long orbits and affects the rate of convergence but not the result of the periodic orbit expressions for the leading eigenvalue and derived quantities. They lead to the two most often used closed expressions for the diffusion constant, one obtained directly from the trace,

$$D = \frac{1}{2d} \lim_{n \rightarrow \infty} \frac{\sum_{\mathbf{x}: \mathbf{f}^n(\mathbf{x})=\mathbf{x}} \Delta \mathbf{x}^2 / |\Lambda|}{\sum_{\mathbf{x}: \mathbf{f}^n(\mathbf{x})=\mathbf{x}} T / |\Lambda|} \quad (73)$$

and one obtained using dynamical zeta functions,

$$D = \frac{1}{2d} \frac{\sum'_{\{p\}} (-1)^k (\Delta \mathbf{x}_1 + \dots + \Delta \mathbf{x}_k)^2 / |\Lambda_1 \dots \Lambda_k|}{\sum'_{\{p\}} (-1)^k (T_1 + \dots + T_k) / |\Lambda_1 \dots \Lambda_k|} \quad (74)$$

Here,  $\Delta \mathbf{x}$  is the displacement of an orbit that is periodic in the elementary cell. It might be zero, corresponding to a periodic orbit in the extended phase space, or it might be nonzero, finishing at an equivalent point on a different scatterer.  $T$  is the period, in terms of the continuous time.  $p$  indicates prime cycles, that is, those periodic orbits that are not repeats of shorter orbits. For the first expression, the sum is over all periodic points, whether belonging to a prime cycle or the repeat of a prime cycle; in the limit  $n \rightarrow \infty$  almost all cycles are prime, so this does not matter. The second expression is a sum over all sets of prime cycles containing  $k = 1, 2, 3 \dots$  cycles. The alternating sign  $(-1)^k$  usually leads to partial cancellations between longer cycles  $AB$  and a combination of shorter cycles that approximate them,  $A$  and  $B$ , thus making the zeta function more rapidly convergent than the trace formula. The zeta function expression is usually ordered by topological length, that is, all combinations of cycles with a total number of collisions less than a maximum  $N_{max}$  are counted, with an assumed limit  $N_{max} \rightarrow \infty$ .

The current is computed by similar expressions (omitting  $2d$  and the powers of two), and in fact any phase variable  $a(\mathbf{x})$  may be averaged in this manner, replacing  $\Delta \mathbf{x}$  by  $\int a dt$  computed along the periodic orbit. The trace formula (73) thus leads to a sequence of increasingly detailed measures supported on the periodic orbits given by Dirac delta functions weighted by the inverse orbit stability. The zeta function expression (74) gives a more complicated but often more quickly convergent (in a weak sense) sequence of measures on the same sets.

There have been a number of applications of the above formulae to the hexagonal Lorentz gas [86, 87, 88, 89] numerically searching for periodic orbits up to typically ten collisions and computing the current or the diffusion coefficient. There are a number of technical difficulties, such as making sure all of the tens of thousands of orbits up to this length are found and making maximal use of the symmetry. The conclusions are that the formulae work, although not yet

to the level of precision of alternative methods; the symbolic dynamics (allowed sequences of collisions) is very complicated and depends strongly on the external field; the trace formula may converge more quickly than the zeta function for this system. A zeta function approach with ordering by stability  $\Lambda_{max}$  rather than topological length  $N_{max}$  appears to work better when there are many almost stable cycles at high field [65] (see Sec. 5.6) and in other systems with weak hyperbolicity [81].

Finally, there are general arguments made using periodic orbit measures confirming a number of physical results. It is clear from (73) that the diffusion coefficient must be nonnegative, in agreement with the second law of thermodynamics. Combining a periodic orbit and its time reverse (with negative displacement and Lyapunov exponents) and using the Lyapunov sum rule (52), it is possible to show that  $\mathbf{J} \cdot \mathbf{F}$  and hence the entropy production (41,48) must also be nonnegative out of equilibrium. This argument was given in Ref. [90] for the Lorentz gas and extended to systems with many particles in Ref. [91]. This leads to the following explanation of the second law in thermostatted systems: periodic orbits corresponding to increasing entropy are more stable and have smaller values of  $\Lambda$  than their time reversed counterparts, hence those with increasing entropy are weighted more strongly, leading to an average entropy production which is nonnegative. Rondoni and Cohen [92] have used periodic orbit measures for thermostatted systems to derive the Onsager reciprocal relations which state that the full linear response matrix connecting all possible fluxes and forces is symmetric.

## 5.6 Nonlinear response

Diffusion in the Lorentz gas is a linear process. In Sec. 3.3 the point particles are noninteracting, so the properties of a distribution of many point particles can be obtained by a linear superposition of many single particle trajectories. Until the noninteracting, pointlike approximation fails, there is no density at which the system ceases to be linear. On the other hand, the nonequilibrium Lorentz gas has a natural scale, determined by when the curvature induced in the trajectories by the field is comparable to the distance between the scatterers, at which the current is no longer approximately proportional to the field.

One approach to nonlinear response is to define nonlinear Burnett coefficients. Linear Burnett coefficients which form an expansion for the particle flux in terms of higher derivatives of the density were briefly described in Sec. 4.3. We could also envisage nonlinear Burnett coefficients forming an expansion for the current in terms of higher powers of the field, or vice versa. In realistic systems such an expansion usually involves nonanalytic terms. For example, in three dimensional shear flow, the viscosity  $\eta$  is well described in terms of the shear rate  $\gamma$  (not too large) by  $\eta = \eta_0 - \eta_1 \gamma^{1/2}$  [30]. The nonequilibrium Lorentz gas is still more problematic, with  $\mathbf{J}$  most likely nondifferentiable almost everywhere, although this has not been proved and numerical evidence is far from conclusive, see Fig. 4. It is also unknown whether the diffusion coefficient is a differentiable function of the spacing between the scatterers. Discontinuous

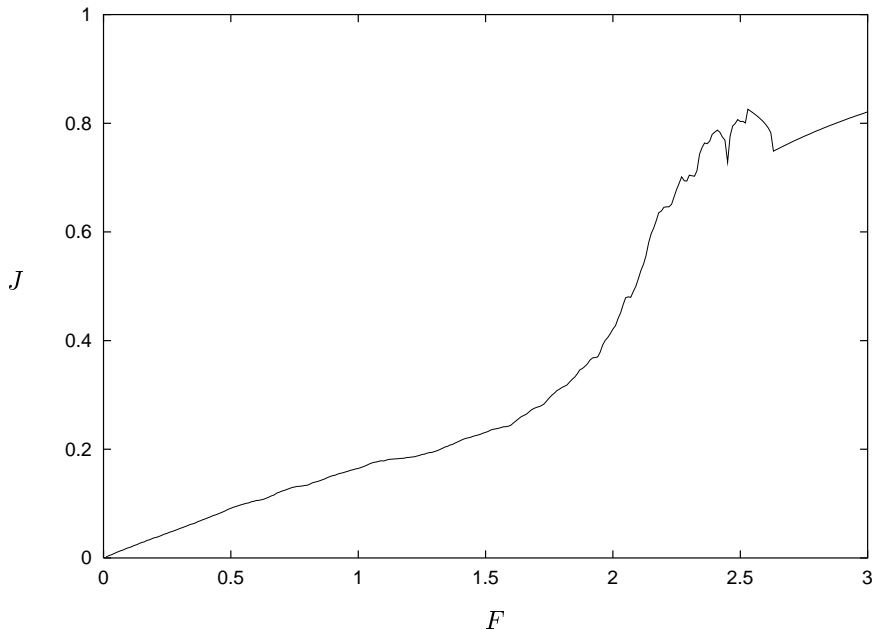


Figure 4: Current versus field for the nonequilibrium Lorentz gas. The lattice is hexagonal with  $w = 0.236$  and finite horizon, see Fig. 3. The field is directed along the line between nearest neighbours. At small field the current is proportional to field according to (49) with a diffusion coefficient of approximately 0.18. The support of the attractor collapses to a fractal set at about  $F = 2.2$ , but this has no apparent effect on the current. For some fields above 2.4 and all fields above about 2.5 the attractor is a stable periodic orbit. The speed of the particle is fixed, so the current can never exceed unity.

one dimensional maps are known to exhibit nondifferentiable diffusion coefficients [93], however the Lorentz gas dynamics viewed as a flow is continuous so the diffusion coefficient is probably somewhat smoother.

We observed in Sec. 4.3 that the symmetry of the hexagonal Lorentz gas requires that an isotropic conductivity, and hence to linear order the average current is parallel to the field. There is no such restriction for the nonlinear response; except for the cases when the field points along the line between nearest or next nearest neighbours (hence a reflection symmetry), the average current is not in general parallel to the field [55].

It is known that for sufficiently small field the two dimensional nonequilibrium Lorentz gas with finite horizon is ergodic [57]. Together with time reversibility and the continuity of the dynamics (in continuous time, not in the Poincaré map), this implies that while almost all initial conditions lead to the same average current, there are arbitrarily large deviations for short times. This is because almost every trajectory must pass arbitrarily close to the time reverse

of a normal trajectory, that is, a trajectory with negative entropy production.

At larger field strengths, the ergodicity is observed to break in one of two ways, depending on the spacing of the scatterers and the orientation of the lattice with respect to the field [94]. One possibility is that a marginally stable periodic orbit appears, surrounded by an elliptic region separate from the rest of the hyperbolic phase space, first observed by Moran and Hoover [53]. If the initial condition is inside this region, the particle always moves between the same two scatterers, and the average current is zero. Outside the region, the dynamics is similar to that at lower fields.

In the other mechanism, the final state (and hence average current) is the same for almost all initial conditions, however it is no longer dense in phase space, and has a box counting dimension less than that of phase space. It is now completely disjoint from its time reverse (the “repeller”), and deviations from the second law are limited to a single collision. This implies that the distribution of fluctuations (both parallel and perpendicular to the field) is quite different to that of small field. The transition to this state, described in Ref. [94] is termed crisis induced intermittency, and corresponds to a discontinuous change in the box counting dimension of the attractor, but the current, Lyapunov exponent, and information dimension are continuous. Not all periodic orbits now lie in the attractor, so it is imperative that periodic orbit calculations (Sec. 5.5) only contain those cycles actually in the attractor. This can be accomplished by searching a long typical trajectory (rather than the whole phase space) for periodic orbits, often a useful approach in any case.

Typically, both mechanisms are observed at different field strengths for the same spacing, and as the field is further increased, further crises occur, creating, destroying and removing periodic orbits from the attractor. Eventually one (or more [95]) periodic orbits becomes stable, attracting all or at least a positive measure of initial conditions. There is a range of fields over which stable windows and chaotic attractors alternate in a complicated fashion [55]. At sufficiently large fields there is always a stable orbit, and at infinite field, the limiting behaviour is that of an orbit creeping along a disk until it can move in the direction of the field to the next disk.

While it is clear that many similar features occur in the three dimensional nonequilibrium Lorentz gas [54] and various molecular dynamics simulations driven to very high fields [30], the details depend to a large extent on the model at hand. While it might require unreasonably strong forcing to generate stable configurations with no positive Lyapunov exponents, it is sufficient to let only one of the positive exponents go negative to expect that the attractor and repeller are disjoint, and therefore a dynamical and time reversible structure qualitatively different to that near equilibrium. It is also possible that measurements of large systems ignore and hence average over many degrees of freedom, which may tend to wash out the multifractal structure of phase space. In any case, there is much more to be understood about the dynamics of a many particle system in a far from equilibrium steady state.

## 6 Boundary driven systems

### 6.1 Open boundaries: The escape rate formalism

Now we turn to nonequilibrium systems with Newtonian equations and no phase space contraction, with nonequilibrium effects generated by the boundaries. Systems with both boundary effects and thermostats are considered in Sec. 6.3.

Suppose we consider a Lorentz gas, either random or periodic (with finite horizon), in a bounded region of space. Trajectories in the system can then be divided into four classes, depending on whether they remain in the system at late or at early times. Almost all (Lebesgue measure) trajectories remain in the system for only a finite time. Those that remain in the system at both early and late times form the repeller, which in this case is the closure of the periodic orbits. Trajectories that are in the system at late but not early times form the stable manifold of the repeller, and those in the system at early but not late times form the unstable manifold of the repeller.

A smooth distribution of initial conditions will converge (weakly) to a distribution over the repeller and its unstable manifold that is steady except that it decays in time as the measure escapes through the boundary. In the language of Sec. 5.5, a generic initial distribution acted on by the Liouville evolution operator will be dominated at late times by its leading eigenfunction. The rate of decay, the escape rate  $\gamma$ , is directly given by the leading eigenvalue; the number of particles in the system given an initial uniform distribution decays as

$$N(t) \sim N(0)e^{-\gamma t} \quad (75)$$

This exponential decay rate and its calculation as an eigenvalue using standard periodic orbit theory [3, 96] depends on the uniform hyperbolicity of the system. Nonuniformly hyperbolic systems have recently been treated in this manner, but with more care due to the appearance of a power law decay and a branch cut in the spectrum [97]. For hyperbolic systems, the escape rate is also related to other dynamical quantities, the sum of the positive Lyapunov exponents, and the Kolmogorov-Sinai entropy by [32]

$$\gamma = \sum \lambda_+ - h_{KS} \quad (76)$$

and in the two dimensional case, also to the partial information codimension  $c_1$  [98]

$$\gamma = \lambda_+ c_1 \quad (77)$$

where  $c_1$  is the dimension of phase space minus the information dimension  $D_1$  of either the stable or the unstable manifold. So far we have related the exponential escape rate of a hyperbolic system to periodic orbits, the positive Lyapunov exponent(s) and a dimension of the repeller.

Suppose now that the dimensions of the system are so large (specifically, much larger than the mean free path) that the evolution of phase space density is well described by the diffusion equation (32). Open square boundaries correspond to the condition  $P = 0$  on  $x = 0$ ,  $y = 0$ ,  $x = L$  and  $y = L$  (for simplicity;

other geometries are possible, altering the constant  $\pi^2$  below), leading to the general solution

$$P(x, y, t) = \sum_{m=1}^{\infty} \sum_{n=1}^{\infty} p_{m,n} \sin \frac{m\pi x}{L} \sin \frac{n\pi y}{L} \exp \left[ -\frac{D\pi^2}{L^2} (m^2 + n^2)t \right] \quad (78)$$

from which we find the decay rate of the leading  $m = n = 1$  mode,

$$\gamma = \frac{2\pi^2 D}{L^2} \quad (79)$$

Equating the escape rates of the dynamical and hydrodynamic approaches in the limit of large systems, we obtain escape rate expressions for the diffusion coefficient [99],

$$D = \lim_{L \rightarrow \infty} \frac{\gamma L^2}{2\pi^2} = \lim_{L \rightarrow \infty} \frac{L^2}{2\pi^2} (\sum \lambda_+ - h_{KS}) = \lim_{L \rightarrow \infty} \frac{L^2}{2\pi^2} \lambda_+ c_1 = \lim_{L \rightarrow \infty} \frac{L^2}{2\pi^2} \lambda_+ c_H \quad (80)$$

where the last equality involving the partial Hausdorff codimension in the large system limit is found in Ref. [100]. This is useful since  $c_H$  can be computed more easily than either  $h_{KS}$  or  $c_1$  [101]. Unfortunately none of the above quantities can be calculated efficiently enough in the large system limit for these equations to compete with the thermostatted approach as a means of computing the diffusion coefficient. They can be used to check the consistency of the approach, however, and remain of great theoretical interest. Compare Eq. (53) where the information codimension in the thermostatted two dimensional Lorentz gas gives a very similar expression for the diffusion coefficient:

$$D = \lim_{F \rightarrow 0} \frac{\lambda_+ c_1}{F^2} \quad (81)$$

Note that the thermostatted Hausdorff codimension is exactly zero up to reasonably strong fields (see Sec. 5.6). The escape rate  $\gamma$  plays the same role for the open system as the multiplier  $\alpha$  plays for the thermostatted system in determining the rate of decay of phase space volume occupied by an initially smooth distribution of particles; in one case particles are lost through the boundaries, while in the other the volume contracts due to the equations of motion.

The escape rate formalism applies not only to diffusion, but also to other linear transport coefficients. The idea is that each Green-Kubo expression (36) can be transformed into an equivalent Einstein relation (35) containing the mean square difference of a quantity other than displacement. Such a quantity is called a Helfand moment, for example, the Helfand moment corresponding to shear viscosity is (up to a constant factor)  $\sum_i x_i p_{iy}$  where the sum is over particles. The escape condition then corresponds to a bound on the Helfand moment. In this way, all linear transport coefficients may be related to escape in an appropriate system with a large size limit. The small size limit corresponds to a steady state far from equilibrium, however it is quite different to the thermostatted system at strong field, and it is not clear what physical system it could represent. More details on the escape rate formalism and its applications can be found in Refs. [6, 7, 99, 100, 102].

## 6.2 Flux boundaries

A Lorentz gas in a finite domain need not have absorbing boundaries; it is also profitable to consider the possibility of injecting particles into the system from the boundaries. The most common (but by no means the only possible) geometry considered for this situation is that of a Lorentz gas (random or periodic with finite horizon) in a slab given by  $-L/2 < x < L/2$  and  $-\infty < y < \infty$ . At the left (right) boundary, particles are injected in all directions with a density  $f_-$  ( $f_+$ ). This is analogous to numerical simulations where boundary conditions at a certain temperature are maintained by injecting particles at the boundary with a Maxwell-Boltzmann distribution, ignoring correlations.

In the steady state, the particles fill the whole phase space except the repeller and its unstable manifold which constitute a set of zero measure. Since phase space volume is conserved, the density of particles at a given position and velocity is either  $f_-$  or  $f_+$  depending on the boundary through which the particles entered. This means that the phase space density is piecewise constant (hence piecewise smooth) with a fractal set where the density is undefined.

This prescription for the phase space density can be coded by the following formula [103]:

$$f(\mathbf{x}, \mathbf{v}) = \frac{f_- + f_+}{2} + \mathbf{g} \cdot \left( \mathbf{x} + \int_0^{-T(\mathbf{x}, \mathbf{v})} \mathbf{v}_t dt \right) \quad (82)$$

where  $\mathbf{g} = \mathbf{e}_x(f_+ - f_-)/L$  is the density gradient across the slab, and  $-T$  is the time the particle entered the system. The term in the large parentheses evaluates to the position the particle entered the system, with an  $x$ -component of  $\pm L/2$ ; combined with  $\mathbf{g}$  it provides the necessary increment to obtain the density  $f_{\pm}$ . The term  $\mathbf{g} \cdot \mathbf{x}$  gives a linear density profile; after integrating over the velocity directions to obtain  $P(\mathbf{x})$  from  $f(\mathbf{x}, \mathbf{v})$ , this is a trivial solution of the diffusion equation (32). The integral then determines how far the actual density  $f_{\pm}$  differs from the average behaviour.

As in Sec. 6.1 above, we are really interested in the large system limit,  $L \rightarrow \infty$ . The gradient  $\mathbf{g}$  is kept finite, while  $f_+ - f_-$  tends to infinity. The first term  $(f_+ + f_-)/2$  can be ignored, as it gives only a constant shift, the average density at  $x = 0$ . The time the particle entered the system goes to  $-\infty$ . We find that the result,

$$\Psi(\mathbf{x}, \mathbf{v}) = \mathbf{g} \cdot \left( \mathbf{x} + \int_0^{-\infty} \mathbf{v}_t dt \right) \quad (83)$$

diverges for all  $\mathbf{x}$  and  $\mathbf{v}$ . This is perhaps not surprising given that the phase space density for the nonequilibrium steady state is multifractal in the thermostatted approach, Sec. 5.3. In any case, it does not cause a problem, since the average with respect to the nonequilibrium distribution  $\langle \rangle_{ne}$  of an arbitrary phase variable  $a(\mathbf{x}, \mathbf{v})$  can be naturally defined by

$$\langle a \rangle_{ne} = \langle a \Psi \rangle = \mathbf{g} \cdot \left( \langle a \mathbf{x} \rangle + \int_0^{-\infty} \langle a \mathbf{v}_t \rangle dt \right) \quad (84)$$

If  $a$  is the current  $\mathbf{J}$ , this leads directly to the expected relation  $\mathbf{J} = -D\mathbf{g}$  with the diffusion coefficient  $D$  given by its Green-Kubo formula (36).

Distributions of this form were originally introduced by Lebowitz [104] and MacLennan [105]. It is possible to represent  $\Psi$  by its cumulative distribution function, which is continuous [6]. It is one of the main tools used to apply Baker maps to the understanding of nonequilibrium steady states and entropy production, where the cumulative distribution function becomes an exactly selfsimilar Takagi function [6, 7, 10]. There is a natural extension to other transport processes in a similar fashion to the open case, Sec. 6.1. See also Ref. [106] where this approach is used to describe hydrodynamics outside local equilibrium.

We conclude our discussion of flux boundary conditions with a connection to the thermostatted approach. Suppose we coarse grain  $\Psi$  to some resolution  $\epsilon$ , ignoring smaller variations. We can approximately compute  $\Psi$  in some region of size  $\epsilon$  in phase space by tracing back in time until the chaotic dynamics amplifies the initial uncertainty to the point at which the particle could have come from any direction with roughly equal probability, time  $-\tau$ . We can then write for the  $\epsilon$  smoothed distribution,

$$\Psi_\epsilon(\mathbf{x}, \mathbf{v}) \approx \mathbf{g} \cdot \mathbf{x}_{-\tau} \quad (85)$$

Compare this with an  $\epsilon$  smoothed distribution using a field and thermostat. For sufficiently small field, the trajectory remains close to a trajectory without field over such a time  $\tau$ . The thermostatted case has no overall variation in density, so the average density at time  $-\tau$  is roughly unity. However, phase space contraction increases the average density to approximately  $e^{\mathbf{F} \cdot \Delta \mathbf{x}}$ , which reduces in the limit of small field to  $1 + \mathbf{F} \cdot \Delta \mathbf{x}$ . Thus the nonequilibrium steady state distribution obtained using flux boundary conditions is the same up to a multiplicative constant as the deviation of the distribution from equilibrium in the weak field thermostatted case. The distribution  $\Psi$  is directly proportional to the gradient  $\mathbf{g}$ , so it cannot exhibit any nonlinear features, as expected for diffusion in the Lorentz gas.

### 6.3 Boundaries with thermostats

There are also a few approaches combining elements from both thermostatted and boundary driven nonequilibrium models. Chernov and Lebowitz [107, 108] use wall collision rules that are energy conserving, time reversible and phase space contracting (on the average) to drive a many particle system into a shearing steady state. This can be made equivalent to a thin layer where the particle is subject to a strong oblique force and a thermostat, and thus belongs with the methods mentioned at the end of Sec. 5.2.

Tél and collaborators [10, 109, 110, 111] consider open systems with an external field. They focus on Baker map approaches, but much of their discussion on the relationships between escape rate, entropy production and dimension applies equally to the Lorentz gas or many particle systems. There are now two limits of interest,  $F \rightarrow 0$  and  $L \rightarrow \infty$ . If the latter is taken first it is

necessary to impose a thermostat to keep the velocity under control. Nevertheless, the phase space contraction is bounded, since the repeller is in a finite domain, see (56). This means that the Lyapunov exponents add to zero as in a Hamiltonian system.

The analysis proceeds similarly to that of the field free case, Sec. 6.1. Eqs. (75-77) pertaining to the escape rate, Lyapunov exponent and the partial information codimension of general open two dimensional systems remain valid. The hydrodynamic equation now contains both a diffusion and drift term,

$$\frac{\partial P}{\partial t} = \nabla \cdot (\overset{\leftrightarrow}{\mathbf{D}} \cdot \nabla P - \mathbf{J}P) \quad (86)$$

where  $\overset{\leftrightarrow}{\mathbf{D}}$  and  $\mathbf{J}$  depend on  $\mathbf{F}$  according to the microscopic dynamics; for the usual case of a homogeneous system  $\mathbf{J}$  does not depend on position. For small field we have  $\mathbf{J} = D\mathbf{F}$  from (49), where  $D$  is the (usually isotropic) zero field diffusion coefficient. The equation is easily solved in a strip  $0 < x < L$  by separation of variables leading to the escape rate

$$\gamma = \frac{D_{xx}\pi^2}{L^2} + \frac{J_x^2}{4D_{xx}} \quad (87)$$

reducing when the zero field limit is taken first to (79) and when the large system limit is taken first to another expression for the diffusion coefficient,

$$D = \lim_{F \rightarrow 0} \frac{4\gamma}{F^2} = \lim_{F \rightarrow 0} \frac{4\lambda_+ c_1}{F^2} \quad (88)$$

The factor of four difference from Eq. (81) was noted in Ref. [110] and is due to the different (here semi-infinite) geometry. In all cases the information codimension of the relevant measure can be associated with the transport coefficient, and hence the entropy production. The thermostatted methods and open systems, alone or in combination, describe the same nonequilibrium processes, at least in the linear regime.

## 7 Outlook

Many of the connections between dynamical and statistical descriptions and between microscopic and macroscopic properties of equilibrium and nonequilibrium stationary states have been addressed using a very simple model, the Lorentz gas. It is remarkable that most of these connections and properties do not depend on the number of particles, but apply to both the smallest and largest systems. There are undoubtedly many more connections to be made on this level. One of the chief aims of the present work is to bring a diversity of ideas together to catalyse progress in this direction. For this purpose, it is also helpful to keep in mind a few limitations of the Lorentz gas paradigm.

In the Lorentz gas it is necessary to distinguish between real space density  $P$  and single particle density  $f$ . Similarly, in many particle systems there is an

additional distinction between single particle density  $f$  and phase space density  $\rho$ . A significant conceptual difficulty is that macroscopic entropy, defined as an extensive quantity according to Sec. 2.2 is a function of real space, while the microscopic descriptions of Sec. 3 involve the phase space. The effect of this, which is not apparent from the Lorentz gas, is that the thermostating multiplier  $\alpha$  and the escape rate  $\gamma$  are not local quantities in general; they depend on a simultaneous description of all the particles. These distinctions are also important with regard to Baker map approaches [10], where concepts such as real space and phase space do not obviously play the same roles and need to be carefully delineated.

There are some instances where the same chaotic properties act differently in larger systems. While we expect systems of many particles to have hyperbolic properties [8], some of the fractal structure might be washed out by measurements that average over many of the degrees of freedom. It is also not clear to what extent such averaging can be simulated by, for example, random placement of the scatterers in the Lorentz gas.

Conversely, some chaotic properties of large systems are different to those of lower dimensional systems. A number of results, particularly those relating dimensions and Lyapunov exponents have only been proven for two dimensional systems. Higher dimensional results may be more difficult to prove, or the structure may be more detailed than in two dimensions. The three dimensional Lorentz gas, corresponding to a five dimensional flow or a four dimensional map and thus having two nontrivial pairs of Lyapunov exponents, has already provided a useful example of the conjugate pairing rule [54] and may well contain much structure characteristic of higher dimensional dynamics. An alternative is the six dimensional map corresponding to three hard disks in two dimensions.

There remain a number of challenges in the theory of stationary states far from equilibrium. Not the least of these is the difficulty defining a useful and unique entropy, despite the observation that the irreversibility of the second law applies universally, near or far from equilibrium. Another issue is that many of the approaches such as various thermostats or boundary conditions are equivalent only in the linear regime. The nonlinear properties of the Lorentz gas given in Sec. 5.6 are only the beginning of what can be understood about such nonequilibrium systems.

The author is grateful for helpful discussions with N. I. Chernov, E. G. D. Cohen, J. R. Dorfman, P. Gaspard and W. G. Hoover, and for collaboration on many of these subjects with G. P. Morriss.

## References

- [1] J. Lebowitz (this volume).
- [2] N. Simányi and D. Szász (this volume).
- [3] P. Cvitanović et al, *Classical and quantum chaos*  
<http://www.nbi.dk/ChaosBook> .

- [4] D. Ruelle, *Statistical mechanics, thermodynamic formalism* (Addison-Wesley, Reading Mass., 1978).
- [5] M. J. Feigenbaum, *J. Stat. Phys.* **19**, 25 (1978).
- [6] P. Gaspard, *Chaos, scattering and statistical mechanics* (Cambridge University, Cambridge UK, 1998).
- [7] J. R. Dorfman, *From molecular chaos to dynamical chaos* (Cambridge University, Cambridge, 1999).
- [8] G. Gallavotti and E. G. D. Cohen, *Phys. Rev. Lett.* **74**, 2694 (1995).
- [9] G. Gallavotti (this volume).
- [10] T. Tél and J. Vollmer (this volume).
- [11] L. Bunimovich (this volume).
- [12] J. L. Lebowitz, *Physics Today* **46**, 32 (1993).
- [13] H. H. Rugh, *Phys. Rev. Lett.* **78**, 772 (1997).
- [14] H. H. Rugh, *J. Phys. A — Math. Gen.* **31**, 7761 (1998).
- [15] G. P. Morriss and L. Rondoni, *Phys. Rev. E* **59**, R5 (1999).
- [16] C. P. Dettmann and G. P. Morriss, *Phys. Rev. E* **54**, 2495 (1996).
- [17] G. Ayton, O. G. Jepps and D. J. Evans, *Mol. Phys.* **96**, 915 (1999).
- [18] H. Spohn, *Large scale dynamics of interacting particles* (Springer-Verlag, New York, 1991).
- [19] H. A. Lorentz, *Proc. Amst. Acad.* **7**, 438 (1905).
- [20] H. van Beijeren, *Rev. Mod. Phys.* **54**, 195 (1982).
- [21] N. A. Metropolis, A. W. Rosenbluth, M. N. Rosenbluth, A. H. Teller and E. Teller, *J. Chem. Phys.* **21**, 1087 (1953).
- [22] N. Chernov, *J. Stat. Phys.* **88**, 1 (1997).
- [23] E. M. Lifshitz and L. P. Pitaevskii, *Physical kinetics* (Pergamon, London, 1981).
- [24] J. R. Dorfman, H. van Beijeren, R. van Zon (this volume).
- [25] M. H. Ernst and A. Weijland, *Phys. Lett. A* **34**, 39 (1971).
- [26] J. M. J. van Leeuwen and A. Weijland, *Physica* **36**, 457 (1967).
- [27] L. E. Reichl, *A modern course in statistical physics* 2nd edition (Wiley, New York, 1998).

- [28] L. Rondoni and E. G. D. Cohen, “Gibbs entropy and irreversible thermodynamics” (preprint).
- [29] M. P. Allen and D. J. Tildersley, *Computer simulation of liquids* (Clarendon, Oxford, 1987).
- [30] D. J. Evans and G. P. Morriss, *Statistical mechanics of nonequilibrium liquids* (Academic, London, 1990).
- [31] W. G. Hoover, *Computational statistical mechanics* (Elsevier, Amsterdam, 1991).
- [32] J.-P. Eckmann and D. Ruelle, *Rev. Mod. Phys.* **57**, 617 (1985).
- [33] D. W. Brenner, *Phys. Rev. B* **42**, 9458 (1990); **46**, 1948 (1992).
- [34] J. D. Weeks, D. Chandler and H. C. Andersen, *J. Chem. Phys.* **54**, 5237 (1971).
- [35] J. Machta and R. Zwanzig, *Phys. Rev. Lett.* **50**, 1959 (1983).
- [36] P. M. Bleher, *J. Stat. Phys.* **66**, 315 (1992).
- [37] P. Dahlqvist, *J. Stat. Phys.* **84**, 773 (1996).
- [38] M. S. Green, *J. Chem. Phys.* **22**, 398 (1954).
- [39] R. Kubo, *J. Phys. Soc. Jpn.* **12**, 570 (1957).
- [40] L.-S. Young, *Ann. Math.* **147**, 585 (1998).
- [41] N. Chernov, *J. Stat. Phys.* **94**, 513 (1999).
- [42] P. Gaspard, *Phys. Rev. E* **53**, 4379 (1996).
- [43] D. J. Evans and S. Sarman, *Phys. Rev. E* **48**, 65 (1993).
- [44] G. Gallavotti, *Physica D* **105**, 163 (1997).
- [45] W. G. Hoover, A. J. C. Ladd and B. Moran, *Phys. Rev. Lett.* **48**, 1818 (1982).
- [46] D. J. Evans, *J. Chem. Phys.* **78**, 3297 (1983).
- [47] G. P. Morriss and C. P. Dettmann, *Chaos* **8**, 321 (1998).
- [48] S. Nosé, *J. Chem. Phys.* **81**, 511 (1984).
- [49] S. Nosé, *Mol. Phys.* **52**, 255 (1984).
- [50] S. Nosé, *Prog. Theor. Phys. Suppl.* **103**, 1 (1991).
- [51] R. van Zon, [cond-mat/9905027](https://arxiv.org/abs/cond-mat/9905027)

- [52] H. A. Posch, W. G. Hoover and F. J. Vesely, *Phys. Rev. A* **33**, 4253 (1986).
- [53] B. Moran and W. G. Hoover, *J. Stat. Phys.* **48**, 709 (1987).
- [54] C. P. Dettmann, G. P. Morriss and L. Rondoni, *Phys. Rev. E* **52**, R5746 (1995).
- [55] J. Lloyd, M. Niemeyer, L. Rondoni and G. P. Morriss, *Chaos* **5**, 536 (1995).
- [56] I. Procaccia, *Phys. Scr.* **T9**, 40 (1985).
- [57] N. I. Chernov, G. L. Eyink, J. L. Lebowitz, Ya. G. Sinai, *Commun. Math. Phys.* **154**, 569 (1993).
- [58] T. Yamada and K. Kawasaki, *Prog. Theor. Phys.* **38**, 1031 (1967).
- [59] D. Ruelle, *J. Stat. Phys.* **85**, 1 (1996).
- [60] D. J. Evans, E. G. D. Cohen and G. P. Morriss, *Phys. Rev. Lett.* **71**, 2401 (1993).
- [61] G. Gallavotti and E. G. D. Cohen, *Phys. Rev. Lett.* **74**, 2694 (1995).
- [62] G. Gallavotti and E. G. D. Cohen, *J. Stat. Phys.* **80**, 1645 (1994).
- [63] C. W. Misner, K. S. Thorne and J. A. Wheeler, *Gravitation* (Freeman, San Francisco, 1973)
- [64] C. P. Dettmann, “Hamiltonian for a restricted isoenergetic thermostat”  
chao-dyn/9906031
- [65] C. P. Dettmann and G. P. Morriss, *Phys. Rev. E*, **55**, 3693 (1997).
- [66] W. G. Hoover, B. Moran, C. G. Hoover and W. J. Evans, *Phys. Lett. A* **133**, 114 (1988).
- [67] P. Choquard, *Chaos* **8**, 350 (1998).
- [68] M. P. Wojtkowski and C. Liverani, *Commun. Math. Phys.* **194**, 47 (1998).
- [69] D. Abraham and J. E. Marsden, *Foundations of mechanics*, 2nd ed. (Benjamin/Cummins, Reading Mass., 1978).
- [70] U. Dressler, *Phys. Rev. A* **38**, 2103 (1988).
- [71] G. P. Morriss, *Phys. Lett. A* **134**, 307 (1988).
- [72] S. Sarman, D. J. Evans and G. P. Morriss, *Phys. Rev. A* **45**, 2233 (1992).
- [73] Ch. Dellago, H. Posch and W. G. Hoover, *Phys. Rev. E* **53**, 1483 (1996).
- [74] D. J. Searles, D. J. Evans and D. J. Isbister, *Chaos* **8**, 337 (1998).

- [75] D. J. Evans, E. G. D. Cohen and G. P. Morriss, Phys. Rev. A **42**, 5990 (1990).
- [76] C. P. Dettmann and G. P. Morriss, Phys. Rev. E **53**, R5545 (1996).
- [77] D. Ruelle, “Smooth dynamics and new theoretical ideas in nonequilibrium statistical mechanics”, `chao-dyn/9812032`
- [78] F. Bonetto, E. G. D. Cohen and C. Pugh, J. Stat. Phys. **92**, 587 (1998).
- [79] R. Artuso, E. Aurell and P. Cvitanović, Nonlinearity **3**, 325 (1990); **3**, 361 (1990).
- [80] H. H. Rugh, Ergodic Theory Dynamical Systems **16**, 805 (1996).
- [81] C. P. Dettmann and P. Dahlqvist, Phys. Rev. E **57**, 5303 (1998).
- [82] M. C. Gutzwiller, *Chaos in classical and quantum mechanics* (Cambridge University, Cambridge, 1993).
- [83] P. Cvitanović, C. P. Dettmann, R. Mainieri and G. Vattay, J. Stat. Phys. **93**, 981 (1998).
- [84] P. Cvitanović, C. P. Dettmann, R. Mainieri and G. Vattay, Nonlinearity **12**, 939 (1999).
- [85] D. Ruelle, J. Stat. Phys. **44**, 281 (1986).
- [86] P. Cvitanović, P. Gaspard and T. Schreiber, Chaos **2**, 85 (1992).
- [87] W. N. Vance, Phys. Rev. Lett. **69**, 1356 (1992).
- [88] G. P. Morriss and L. Rondoni, J. Stat. Phys. **75**, 553 (1994).
- [89] P. Cvitanović, J.-P. Eckmann and P. Gaspard, Chaos Solitons Fractals **6**, 113 (1995).
- [90] C. P. Dettmann, G. P. Morriss and L. Rondoni, Chaos Solitons Fractals **8**, 783 (1997).
- [91] L. Rondoni and G. P. Morriss, J. Stat. Phys. **86**, 991 (1997).
- [92] L. Rondoni and E. G. D. Cohen, Nonlinearity **11**, 1395 (1998).
- [93] R. Klages and J. R. Dorfman, Phys. Rev. Lett. **74**, 387 (1995).
- [94] C. P. Dettmann and G. P. Morriss, Phys. Rev. E **54**, 4782 (1996).
- [95] G. P. Morriss, private communication.
- [96] L. Kadanoff and C. Tang, Proc. Natl. Acad. Sci. USA, **81**, 1276 (1984).
- [97] P. Dahlqvist, `chao-dyn/9903025`

- [98] L. S. Young, *Ergod. Th. and Dyn. Syst.* **2**, 109 (1982).
- [99] P. Gaspard and G. Nicolis, *Phys. Rev. Lett.*, **65**, 1693 (1990).
- [100] P. Gaspard and F. Baras, *Phys. Rev. E* **51**, 5332 (1995).
- [101] E. Ott, *Chaos in dynamical systems* (Cambridge University, Cambridge, 1993).
- [102] P. Gaspard and J. R. Dorfman, *Phys. Rev. E* **52**, 3525 (1995).
- [103] P. Gaspard, *Physica A* **240**, 54 (1997).
- [104] J. L. Lebowitz, *Phys. Rev.* **114**, 1192 (1959).
- [105] J. A. MacLennan, Jr., *Phys. Rev.* **115**, 1405 (1959).
- [106] G. L. Eyink, J. L. Lebowitz and H. Spohn, *J. Stat. Phys.* **83**, 385 (1996).
- [107] N. I. Chernov and J. L. Lebowitz, *J. Stat. Phys.* **86**, 953 (1997).
- [108] F. Bonetto, N. I. Chernov and J. L. Lebowitz, *Chaos* **8**, 823 (1998).
- [109] W. Breyermann, T. Tél and J. Vollmer, *Phys. Rev. Lett.* **77**, 2945 (1996).
- [110] J. Vollmer, T. Tél and W. Breyermann, *Phys. Rev. Lett.* **79**, 2759 (1997).
- [111] J. Vollmer, T. Tél and W. Breyermann, *Phys. Rev. E* **58**, 1672 (1998).